

# NASA TECHNICAL NOTE



**NASA TN D-5919**

*c. 1*

NASA TN D-5919

LOAN COPY: RETU  
AFWL (WL0L)  
KIRTLAND AFB, N

0132792



TECH LIBRARY KAFB, NM

## AN ANALYSIS OF THE EFFECT OF DESIGN AND MEASUREMENT ERRORS ON PUMP PERFORMANCE PARAMETERS

*by Douglas A. Anderson*

*Lewis Research Center*

*Cleveland, Ohio 44135*



0132792

1. Report No. NASA TN D-5919	2. Government Accession No.	3. Recipient's Catalog No.	0132792	
4. Title and Subtitle AN ANALYSIS OF THE EFFECT OF DESIGN AND MEASUREMENT ERRORS ON PUMP PERFORMANCE PARAMETERS		5. Report Date July 1970		
7. Author(s) Douglas A. Anderson		6. Performing Organization Code		
9. Performing Organization Name and Address Lewis Research Center National Aeronautics and Space Administration Cleveland, Ohio 44135		8. Performing Organization Report No. E-4704		
12. Sponsoring Agency Name and Address National Aeronautics and Space Administration Washington, D. C. 20546		10. Work Unit No. 128-31		
15. Supplementary Notes		11. Contract or Grant No.		
16. Abstract  Equations and carpet plots are presented which can be used for determining the effects of design and measurement errors on pump performance parameters. The design error equations apply to a blade element design procedure. The measurement error equations apply to pump tests in which radial surveys of pressure and angle measurements are made. Applications of the error analysis techniques are discussed. The effects of changes in stagger angle and loading on the sensitivity of the performance parameters to design and measurement errors are deduced.		13. Type of Report and Period Covered Technical Note		
17. Key Words (Suggested by Author(s)) Pump Measurement errors Design errors Uncertainty interval		18. Distribution Statement Unclassified - unlimited		
19. Security Classif. (of this report) Unclassified	20. Security Classif. (of this page) Unclassified	21. No. of Pages 65	22. Price* \$3.00	

\*For sale by the Clearinghouse for Federal Scientific and Technical Information  
Springfield, Virginia 22151

# AN ANALYSIS OF THE EFFECT OF DESIGN AND MEASUREMENT ERRORS ON PUMP PERFORMANCE PARAMETERS

by Douglas A. Anderson  
Lewis Research Center

## SUMMARY

A method is presented for calculating the effects of design and measurement errors on pump performance parameters. Error equations and charts are presented which relate the amount of error in a given performance parameter to the amount of error in a given design or measured variable. The design error equations were developed for a blade element design procedure. The measurement error equations apply to pump tests in which radial surveys of pressure and angle measurements are made.

Some specific applications of the error analysis equations are discussed. The computed error values provide a criterion of how large a change in a performance parameter must be to be considered significant. This is useful when comparing design performance to measured performance or when comparing the measured performance of different pumps. The error equations may also be used to determine the sensitivity of a given design to design errors and manufacturing tolerances, or to assess the relative importance of several measurement errors in a particular test configuration. The applications often require that the effect of two or more errors on a given performance parameter be considered. This is done by using the concept of the uncertainty interval, which is explained in this report. Finally, an example is given which demonstrates the application of the measurement error analysis to some typical test data.

Some general trends of the sensitivity of the performance parameters to design and measurement errors were deduced. The sensitivity to design errors generally increased with increasing stagger angle or decreasing loading. For measurement errors, no general trends with stagger angle or loading were indicated.

The error equations were developed for axial flow rotors, but are not limited to this type of blade row. Modifications to the equations are presented which allow them to be applied to stators. Another modification is mentioned which allows them to be applied to mixed-flow impellers.

## INTRODUCTION

The importance of measurement errors in a pump test program is generally recognized. In fact, it would be hard to evaluate any set of test data without developing some intuitive feeling about the effect of errors. However, mathematical techniques are available which allow a methodical analysis of the effect of measurement errors on the resulting flow and performance parameters. Using these techniques, the amount of error to be expected in the performance parameters can be calculated from estimates of the errors introduced by the different measurements. An error analysis can also be of use in planning instrumentation by showing which measurement is likely to introduce the largest errors.

An analysis of the effect of errors should also be useful in a pump design system. Such an analysis would show the sensitivity of a given design to design errors and manufacturing tolerances. It would allow estimates of design precision, the limits around the design point within which the pump performance may be expected to lie with reasonable certainty. Also, an error analysis would show which step in a design procedure is the most critical source of error. These examples show just a few of the applications of an error analysis to pump design procedures and test results.

An error analysis was developed in reference 1 and applied to axial flow compressors. Equations were derived which relate the amount of error in a given compressor performance parameter to the amount of error in a selected design variable or measured variable. The methods used herein to derive the error equations for axial flow pumps are the same as used in reference 1, but almost all of the derived error equations are different. They are different because different parameters are used to describe pump performance, due to the incompressibility of the pump flow, and the effect of cavitation. Further differences between the pump and compressor error analyses arise because of different ranges of interest for some parameters (e. g. , blade stagger angle and flow coefficient) and slightly different measurement techniques.

The purpose of this report is to present the methods which can be used to calculate the effects of both design errors and measurement errors on pump performance. Equations are derived which relate the amount of error in a given pump performance parameter to the amount of error assumed in a given design or measured variable. These equations apply to flow along streamlines or along blade elements. The equations are presented in the form of carpet plots. Whenever feasible, the pump error analysis is presented in a manner similar to that of reference 1. Some uses of the error analysis equations are suggested. The effects of changes in stagger angle and loading on the sensitivity of the performance parameters to design and measurement errors are discussed. An example is given in which the measurement error equations are applied to some typical pump test data.

## DERIVATION OF EQUATIONS

### General Error Analysis Equations

Consider a function of  $n$  variables,  $f(x_1, x_2, \dots, x_n)$ . The change in  $f$  due to a small change in one of the variables  $x_m$  is given approximately by

$$\Delta f_m = \frac{\partial f}{\partial x_m} \Delta x_m \quad (1)$$

(Symbols are defined in appendix A.) If the error in each variable  $x_1, x_2, \dots, x_n$  is known, the resulting error in the function  $f$  can be computed from

$$\Delta f = \frac{\partial f}{\partial x_1} \Delta x_1 + \frac{\partial f}{\partial x_2} \Delta x_2 + \dots + \frac{\partial f}{\partial x_n} \Delta x_n \quad (2)$$

where  $\Delta$  denotes a known or calculated value of the respective error. This equation can be used for systematic errors, which are errors of known sign and approximately known magnitude.

However, the errors encountered in the design and measurement analyses are more likely to be of the type called random errors or uncertainties. Reference 2 discusses the nature of these uncertainties and how they should be treated statistically. (Uncertainty, as defined in ref. 2, is the more precise term.) The relative size of the error or uncertainty can be given in terms of an uncertainty interval as used in references 1 and 2. If, for example, for a measured pressure of 50 psi, there is an estimated 90 percent probability that the true pressure is between 49 and 51 psi, the uncertainty interval is 2 psi for this probability. If the uncertainty intervals of the other measured variables at the same probability are known, the uncertainty interval of the parameter  $f$  for this probability can be computed from

$$(\Delta f)^2 = \left( \frac{\partial f}{\partial x_1} \Delta x_1 \right)^2 + \left( \frac{\partial f}{\partial x_2} \Delta x_2 \right)^2 + \dots + \left( \frac{\partial f}{\partial x_n} \Delta x_n \right)^2 \quad (3)$$

In this equation,  $\Delta$  refers to an uncertainty interval. (Except for a difference in notation, this is the same as eq. (7) of ref. 2.) It is assumed that all of the errors  $\Delta x_1, \Delta x_2$ , etc., have a normal distribution, but the equation is sufficiently accurate for any distribution likely to occur. It is also assumed that the variables  $x_1, x_2$ , etc., are independent; that is, a change in one will have no effect on the values of the others.

It is often more convenient to deal with dimensionless terms  $\Delta f/f$ ,  $\Delta x_1/x_1$ , etc. These terms are easily expressed as percentage errors, and a simplified form of the error equations often results. Using dimensionless terms, equation (2) for systematic errors might become

$$\frac{\Delta f}{f} = \left( \frac{x_1}{f} \frac{\partial f}{\partial x_1} \right) \frac{\Delta x_1}{x_1} + \left( \frac{1}{f} \frac{\partial f}{\partial x_2} \right) \Delta x_2 + \dots \quad (4)$$

This equation shows the error  $\Delta x_1/x_1$  in dimensionless form, but not  $\Delta x_2$ . The modified error equations will generally have a mixture of both forms. The form  $\Delta x$  is better for angles, but the dimensionless form,  $\Delta x/x$ , is usually more convenient for all other variables. The corresponding equation for random errors (eq. (3) modified) is

$$\left( \frac{\Delta f}{f} \right)^2 = \left[ \left( \frac{x_1}{f} \frac{\partial f}{\partial x_1} \right) \frac{\Delta x_1}{x_1} \right]^2 + \left[ \left( \frac{1}{f} \frac{\partial f}{\partial x_2} \right) \Delta x_2 \right]^2 + \dots \quad (5)$$

## Design Errors

The design error analysis was developed for a blade element design procedure such as is discussed in reference 3. In a blade element design procedure, the hydrodynamic design (calculation of velocity diagrams and performance parameters) is conducted along selected blade elements. Blade sections to achieve the desired performance are then selected. In a design procedure, certain quantities, which shall be called the design variables, are chosen by the designer or determined from appropriate design correlations. The design variables selected for this analysis are

- Inlet and outlet radius,  $r_1$  and  $r_2$
- Inlet and outlet axial velocity,  $V_{Z1}$  and  $V_{Z2}$
- Wheel speed at the tip,  $U_t$
- Inlet total head,  $H_1$
- Inlet flow angle,  $\beta_1$
- Outlet relative flow angle or deviation angle ( $\beta_2'$  or  $\delta$ )
- Loss coefficient,  $\bar{\omega}$

From the design variables, the pump performance parameters are computed using the design equations (eqs. (B1) to (B12), appendix B). The performance parameters included in the design error analysis are

Inlet and outlet velocities,  $V_1$  and  $V_2$   
 Inlet relative flow angle or incidence angle,  $\beta'_1$  or  $i$   
 Outlet flow angle,  $\beta_2$   
 Ideal head-rise coefficient,  $\psi_i$   
 Head-rise coefficient,  $\psi$   
 Blade element efficiency,  $\eta$   
 Diffusion factor,  $D$

Although  $\Delta H_i$  and  $\Delta H$  are often used instead of  $\psi_i$  and  $\psi$ , they are not included among the performance parameters, since the percentage errors are the same for  $\Delta H_i$  and  $\psi_i$ , and for  $\Delta H$  and  $\psi$ ; that is,  $\Delta(\Delta H_i)/\Delta H_i = \Delta\psi_i/\psi_i$  and  $\Delta(\Delta H)/\Delta H = \Delta\psi/\psi$ .

The values of the design variables, together with their inherent inaccuracies, are the necessary inputs required to do an error analysis of a design procedure. The values of the design variables  $V_{Z1}$ ,  $\beta_1$ , and  $H_1$  are known for selected values of  $r_1$  from the analysis of the flow through the previous blade row or, for the first stage rotor, from the analysis of the flow through the pump inlet. The errors in  $V_{Z1}$ ,  $\beta_1$ , and  $H_1$  are the result of the accumulation of errors in all upstream blade rows. To estimate the errors in the design variables  $\delta$ ,  $\bar{\omega}$ ,  $r_2$ , and  $V_{Z2}$ , which are obtained from correlations with other parameters (e.g., the  $\bar{\omega}$  against  $D$  correlation, radial equilibrium equation, etc.) requires consideration of both the errors in these other parameters and the accuracy of the correlations used. As blade elements should ideally lie along streamlines, any difference between an assumed or calculated  $r_2$  value and that of a streamline through the corresponding inlet radius is regarded as an error in  $r_2$ .

The design variable  $H_1$  is not included in the design error formulas, since none of the performance parameters depend directly on  $H_1$ . No equations are given for design errors in  $r_1$ , as  $r_1$  is regarded as a selected, nonvarying input. Errors in  $U_t$  are regarded as measurement errors rather than design errors and consequently are not included in the design error formulas. However, a designer may wish to include their effect in estimates of design precision (how closely the actual performance is expected to meet the design specifications).

For systematic design errors, the error in a particular performance parameter  $f$  is given by

$$\begin{aligned} \frac{\Delta f}{f} = & \left( \frac{V_{Z1}}{f} \frac{\partial f}{\partial V_{Z1}} \right) \frac{\Delta V_{Z1}}{V_{Z1}} + \left( \frac{1}{f} \frac{\partial f}{\partial \beta_1} \right) \Delta \beta_1 + \left( \frac{V_{Z2}}{f} \frac{\partial f}{\partial V_{Z2}} \right) \frac{\Delta V_{Z2}}{V_{Z2}} + \left( \frac{1}{f} \frac{\partial f}{\partial \beta'_2} \right) \Delta \beta'_2 \\ & + \left( \frac{1}{f} \frac{df}{d\bar{\omega}} \right) \Delta \bar{\omega} + \left( \frac{r_2}{f} \frac{\partial f}{\partial r_2} \right) \frac{\Delta r_2}{r_2} \end{aligned} \quad (6)$$

This is simply equation (4) with  $x_1$ ,  $x_2$ , etc., identified as appropriate design variables. For the case of random errors, the uncertainty interval in  $f$  is related to the uncertainty intervals in the design variables by

$$\begin{aligned} \left(\frac{\Delta f}{f}\right)^2 = & \left[ \left( \frac{V_{Z1}}{f} \frac{\partial f}{\partial V_{Z1}} \right) \frac{\Delta V_{Z1}}{V_{Z1}} \right]^2 + \left[ \left( \frac{1}{f} \frac{\partial f}{\partial \beta_1} \right) \Delta \beta_1 \right]^2 + \left[ \left( \frac{V_{Z2}}{f} \frac{\partial f}{\partial V_{Z2}} \right) \frac{\Delta V_{Z2}}{V_{Z2}} \right]^2 + \left[ \left( \frac{1}{f} \frac{\partial f}{\partial \beta_2'} \right) \Delta \beta_2' \right]^2 \\ & + \left[ \left( \frac{1}{f} \frac{\partial f}{\partial \bar{\omega}} \right) \Delta \bar{\omega} \right]^2 + \left[ \left( \frac{r_2}{f} \frac{\partial f}{\partial r_2} \right) \frac{\Delta r_2}{r_2} \right]^2 \end{aligned} \quad (7)$$

These equations were derived assuming that the design variables are independent. However, in most design systems some of the design variables are interrelated ( $\bar{\omega}$ ,  $D$  correlation, etc.) so that an error in one may provide errors in some of the others. The analysis of such interactions is beyond the scope of this report. However, the effects of these interactions should be small compared with the direct effects of design errors with one exception. The outlet axial velocity  $V_{Z2}$  is strongly affected by the values of  $\beta_2'$  and  $\bar{\omega}$  through the radial equilibrium equation.

The treatment of the variable  $r_2$  requires careful consideration. Like all of the other variables considered in the error analysis,  $r_2$  will have a certain amount of error. But as the outlet design and performance parameters are usually specified or calculated at given values of  $r_2$ , it is not convenient to have to deal with errors in  $r_2$ . Errors in  $r_2$  are especially troublesome if the calculations are to be extended downstream to subsequent blade rows. One remedy is to modify the error values assigned to the other parameters to include the effects of uncertainties in  $r_2$ . Then  $r_2$  can be treated as if its values were fixed.

Assume that a streamline, nominally at radius  $r_2$ , is actually at radius  $r_2 + \Delta r_2$ . The error in  $f$  at  $r_2 + \Delta r_2$  would be given by the appropriate equation (eqs. (2) to (7)) except that the  $\Delta r_2$  term would be zero. Since  $V_{Z2}$ ,  $\beta_2'$ , and  $\bar{\omega}$  are the only design variables affected by a change in  $r_2$ , the value of  $f$  at  $r_2$  is related to the value of  $f$  at  $r_2 + \Delta r_2$  by

$$f(r_2) = f(r_2 + \Delta r_2) - \left( \frac{\partial f}{\partial V_{Z2}} \frac{dV_{Z2}}{dr_2} + \frac{\partial f}{\partial \beta_2'} \frac{d\beta_2'}{dr_2} + \frac{\partial f}{\partial \bar{\omega}} \frac{d\bar{\omega}}{dr_2} \right) \Delta r_2 \quad (8)$$

where  $dV_{Z2}/dr_2$  simply refers to the slope of the graph of  $V_{Z2}$  plotted against  $r_2$ , and similarly for  $\beta_2'$ ,  $\bar{\omega}$ , and  $f$ . From the definition of the total derivative,



$$\frac{df}{dr_2} = \frac{\partial f}{\partial r_2} + \frac{\partial f}{\partial V_{Z2}} \frac{dV_{Z2}}{dr_2} + \frac{\partial f}{\partial \beta'_2} \frac{d\beta'_2}{dr_2} + \frac{\partial f}{\partial \bar{\omega}} \frac{d\bar{\omega}}{dr_2} \quad (9)$$

Thus, the following equation is equivalent to equation (8),

$$f(r_2) = f(r_2 + \Delta r_2) + \left( \frac{\partial f}{\partial r_2} - \frac{df}{dr_2} \right) \Delta r_2 \quad (10)$$

Consequently, to get the correct value of  $\Delta f$  (if the value of  $r_2$  is to be regarded as fixed),  $\partial f / \partial r_2$  in equations (2) to (7) should be replaced by

$$-\left( \frac{\partial f}{\partial V_{Z2}} \frac{dV_{Z2}}{dr_2} + \frac{\partial f}{\partial \beta'_2} \frac{d\beta'_2}{dr_2} + \frac{\partial f}{\partial \bar{\omega}} \frac{d\bar{\omega}}{dr_2} \right)$$

or the equivalent expression

$$\frac{\partial f}{\partial r_2} - \frac{df}{dr_2}$$

The resulting error equations are

(1) For systematic errors and a fixed  $r_2$  value (using dimensionless terms as in eq. (6)),

$$\begin{aligned} \frac{\Delta f}{f} = & \left( \frac{V_{Z1}}{f} \frac{\partial f}{\partial V_{Z1}} \right) \frac{\Delta V_{Z1}}{V_{Z1}} + \left( \frac{1}{f} \frac{\partial f}{\partial \beta_1} \right) \Delta \beta_1 + \left( \frac{V_{Z2}}{f} \frac{\partial f}{\partial V_{Z2}} \right) \frac{\Delta V_{Z2}}{V_{Z2}} + \left( \frac{1}{f} \frac{\partial f}{\partial \beta'_2} \right) \Delta \beta'_2 + \left( \frac{1}{f} \frac{\partial f}{\partial \bar{\omega}} \right) \Delta \bar{\omega} \\ & + \frac{1}{f} \left( \frac{\partial f}{\partial r_2} - \frac{df}{dr_2} \right) \Delta r_2 \end{aligned} \quad (11)$$

(2) For random errors and a fixed  $r_2$  value,

$$\begin{aligned} \left( \frac{\Delta f}{f} \right)^2 = & \left[ \left( \frac{V_{Z1}}{f} \frac{\partial f}{\partial V_{Z1}} \right) \frac{\Delta V_{Z1}}{V_{Z1}} \right]^2 + \left[ \left( \frac{1}{f} \frac{\partial f}{\partial \beta_1} \right) \Delta \beta_1 \right]^2 + \left[ \left( \frac{V_{Z2}}{f} \frac{\partial f}{\partial V_{Z2}} \right) \frac{\Delta V_{Z2}}{V_{Z2}} \right]^2 + \left[ \left( \frac{1}{f} \frac{\partial f}{\partial \beta'_2} \right) \Delta \beta'_2 \right]^2 + \left[ \left( \frac{1}{f} \frac{\partial f}{\partial \bar{\omega}} \right) \Delta \bar{\omega} \right]^2 \\ & + \left[ \frac{1}{f} \left( \frac{\partial f}{\partial r_2} - \frac{df}{dr_2} \right) \Delta r_2 \right]^2 \end{aligned} \quad (12)$$

The replacement of  $\partial f/\partial r_2$  by  $[(\partial f/\partial r_2) - (df/dr_2)]$  should not be considered as a substitution, and the two expressions are not equivalent. Equations (6) and (7) are for an  $r_2$  which has an error  $\Delta r_2$  while equations (11) and (12) are correct for a fixed  $r_2$ .

## Measurement Errors

The measurement error analysis applies to a pump test in which radial surveys of total and static pressure and of flow angle measurements are made, as was done in references 4 and 5. The measured variables considered in this analysis are

- Inlet and outlet velocity,  $V_1$  and  $V_2$
- Inlet and outlet flow angle,  $\beta_1$  and  $\beta_2$
- Inlet and outlet radius,  $r_1$  and  $r_2$
- Net positive suction head,  $H_{sv}$
- Head rise,  $\Delta H$
- Tip speed,  $U_t$

Velocity is not a directly measured quantity, but is computed from the measured value of velocity head. However, it is more convenient to use velocity in the error equations, and the percentage error in velocity is simply half the percentage error in velocity head. When velocity head is measured directly, as done in references 4 and 5, the accuracy is much better than if the velocity head were obtained from separate measurements of total pressure and static pressure.

From the measured variables, the pump performance parameters are calculated from appropriate equations (eqs. (B46) to (B56)). The performance parameters included in this analysis are

- Inlet and outlet flow coefficient,  $\phi_1$  and  $\phi_2$
- Inlet and outlet relative velocity,  $V'_1$  and  $V'_2$
- Inlet relative flow angle or incidence angle,  $\beta'_1$  or  $i$
- Outlet relative flow angle or deviation angle,  $\beta'_2$  or  $\delta$
- Head-rise coefficient,  $\psi$
- Ideal head-rise coefficient,  $\psi_i$
- Blade element efficiency,  $\eta$
- Loss coefficient,  $\bar{\omega}$
- Diffusion factor,  $D$
- Cavitation number,  $k$

The variables  $V_{Z1}$ ,  $V_{Z2}$ ,  $\Delta H$ , and  $\Delta H_i$  are not included in the performance parameters, since their percentage errors are the same as for  $\phi_1$ ,  $\phi_2$ ,  $\psi$ , and  $\psi_i$ , respectively, except when caused by errors in  $U_t$ . An error in  $U_t$  does not affect the accuracy of the values of  $V_{Z1}$ ,  $V_{Z2}$ , and  $\Delta H$ , but the error in  $\Delta H_i$  is given by

$$\Delta(\Delta H_i)/\Delta H_i = -\Delta\psi_i/\psi_i.$$

The measurement error equations (eqs. (B57) to (B93)) relate the amount of error in a given performance parameter to the amount of error in a given measured variable. They are derived from equations (B46) to (B56) in appendix B.

There are a number of factors which cause measurements errors. One is the inherent errors of the instrumentation and data recording systems. The error estimates given in many data reports consider only this source of error. However, in addition to this, the effects of pressure and flow fluctuations, cavitation, etc., on the pressure and angle measurements must be considered. Also, the values of  $r_1$  and  $r_2$  may be in error due to inaccuracies in probe positioning.

Since blade element test data are generally presented as plots of the measured variables and performance parameters against  $r_1$  or  $r_2$ , it would be preferable not to have any uncertainties in these variables. This can be done if the errors in the other parameters are modified to account for the errors in  $r_1$  and  $r_2$ , using the method developed in the design error section of this report. The error in a calculated performance parameter  $f$  due to an error in radial probe position is given by

$$\Delta f = \left( \frac{\partial f}{\partial r} - \frac{df}{dr} \right) \Delta r = - \left( \frac{\partial f}{\partial x_1} \frac{dx_1}{dr} + \frac{\partial f}{\partial x_2} \frac{dx_2}{dr} + \dots \right) \Delta r \quad (13)$$

where  $r$  stands for either  $r_1$  or  $r_2$ . The total derivative  $df/dr$  is simply the slope of the curve of  $f$  plotted against  $r$ . The resulting error equations are

(1) For systematic measurement errors, where  $r_1$  and  $r_2$  are regarded as fixed values

$$\begin{aligned} \frac{\Delta f}{f} = & \left( \frac{V_1}{f} \frac{\partial f}{\partial V_1} \right) \frac{\Delta V_1}{V_1} + \left( \frac{1}{f} \frac{\partial f}{\partial \beta_1} \right) \Delta \beta_1 + \left( \frac{V_2}{f} \frac{\partial f}{\partial V_2} \right) \frac{\Delta V_2}{V_2} + \left( \frac{1}{f} \frac{\partial f}{\partial \beta_2} \right) \Delta \beta_2 + \left( \frac{U_t}{f} \frac{\partial f}{\partial U_t} \right) \frac{\Delta U_t}{U_t} \\ & + \left( \frac{\Delta H}{f} \frac{\partial f}{\partial \Delta H} \right) \frac{\Delta(\Delta H)}{\Delta H} + \left( \frac{1}{f} \frac{\partial f}{\partial H_{sv}} \right) \Delta H_{sv} - \frac{1}{f} \left( \frac{\partial f}{\partial V_1} \frac{dV_1}{dr_1} + \frac{\partial f}{\partial \beta_1} \frac{d\beta_1}{dr_1} + \frac{\partial f}{\partial H_{sv}} \frac{dH_{sv}}{dr_1} \right) \Delta r_1 \\ & - \frac{1}{f} \left( \frac{\partial f}{\partial V_2} \frac{dV_2}{dr_2} + \frac{\partial f}{\partial \beta_2} \frac{d\beta_2}{dr_2} + \frac{\partial f}{\partial H_2} \frac{dH_2}{dr_2} \right) \Delta r_2 \end{aligned} \quad (14)$$

(2) For random measurement errors, where  $r_1$  and  $r_2$  are regarded as fixed values

$$\begin{aligned}
\left(\frac{\Delta f}{f}\right)^2 = & \left[ \left( \frac{V_1}{f} \frac{\partial f}{\partial V_1} \right) \frac{\Delta V_1}{V_1} \right]^2 + \left[ \left( \frac{1}{f} \frac{\partial f}{\partial \beta_1} \right) \Delta \beta_1 \right]^2 + \left[ \left( \frac{V_2}{f} \frac{\partial f}{\partial V_2} \right) \frac{\Delta V_2}{V_2} \right]^2 + \left[ \left( \frac{1}{f} \frac{\partial f}{\partial \beta_2} \right) \Delta \beta_2 \right]^2 \\
& + \left[ \left( \frac{U_t}{f} \frac{\partial f}{\partial U_t} \right) \frac{\Delta U_t}{U_t} \right]^2 + \left[ \left( \frac{\Delta H}{f} \frac{\partial f}{\partial \Delta H} \right) \frac{\Delta(\Delta H)}{\Delta H} \right]^2 + \left[ \left( \frac{1}{f} \frac{\partial f}{\partial H_{sv}} \right) \Delta H_{sv} \right]^2 \\
& + \left[ \frac{1}{f} \left( \frac{\partial f}{\partial V_1} \frac{dV_1}{dr_1} + \frac{\partial f}{\partial \beta_1} \frac{d\beta_1}{dr_1} + \frac{\partial f}{\partial H_{sv}} \frac{dH_{sv}}{dr_1} \right) \Delta r_1 \right]^2 \\
& + \left[ \frac{1}{f} \left( \frac{\partial f}{\partial V_2} \frac{dV_2}{dr_2} + \frac{\partial f}{\partial \beta_2} \frac{d\beta_2}{dr_2} + \frac{\partial f}{\partial H_2} \frac{dH_2}{dr_2} \right) \Delta r_2 \right]^2
\end{aligned} \tag{15}$$

It is also correct to use

$$\frac{1}{f} \left( \frac{\partial f}{\partial r_1} - \frac{df}{dr_1} \right) \Delta r_1$$

and

$$\frac{1}{f} \left( \frac{\partial f}{\partial r_2} - \frac{df}{dr_2} \right) \Delta r_2$$

In the measurement error equations presented for  $\Delta f/\Delta r$  in appendix B, the form is used which is judged most convenient for calculations. However, since  $r_1$  and  $r_2$  are usually changed together, it is not possible to determine the individual values of  $df/dr_1$  and  $df/dr_2$  from a graphically determined value of  $df/dr$ . The value of  $df/dr$  may be used for  $df/dr_2$  if  $f$  is not a function of  $r_1$  or for  $df/dr_1$  if  $f$  is not a function of  $r_2$ . For radially constant inlet total pressure, which is a normal test condition for inlet stages,  $dH_2/dr_2$  can be replaced by  $d\Delta H/dr_2$ .

## Presentation of Equations

The error equations and the equations from which they are derived are listed in appendix B. The equations are presented in the form judged most convenient for use in

TABLE I. - CLASSIFICATION OF THE ERROR EQUATIONS AND CARPET PLOTS  
 ACCORDING TO PERFORMANCE PARAMETER AND DESIGN OR  
 MEASURED VARIABLE

(a) Design errors

Design performance parameters	Design variables										
	$V_{Z1}$		$\beta_1$		$V_{Z2}$		$\beta'_2$ or $\delta$		$\bar{\omega}$	$r_2$	
	Eq.	Fig.	Eq.	Fig.	Eq.	Fig.	Eq.	Fig.	Eq.	Eq.	Fig.
$V_1$	B13	---	B14	1	---	---	---	---	---	---	-----
$V_2$	---	---	---	-----	B15	2(a)	B16	2(b)	---	B17	2(c)
$\beta'_1$	B18	3(a)	B19	3(b)	---	---	---	---	---	---	-----
$\beta_2$	---	---	---	-----	B20	3(a)	B21	3(b)	---	B22	3(a)
$\psi_i$	B23	---	B25	4(a)	B26	4(b)	B28	4(c)	---	B29	4(d)
$\psi$	B30	5(a)	B31	4(a), 5(b)	B32	4(b)	B32	4(c)	B33	B32	4(d)
$\eta$	B34	2(a)	B35	2(b), 4(a)	B36	4(b)	B36	4(c)	B37	B36	4(d)
D	B38	6(a)	B3 <sup>c</sup>	6(b)	B40	6(c)	B41	6(d)	---	B42	7(a), (b)

(b) Measurement errors

Measured performance parameter	Measured variables															
	$V_1$		$\beta_1$		$V_2$		$\beta_2$		$r_1$		$r_2$		$U_t$		$\Delta H$	$H_{sv}$
	Eq.	Fig.	Eq.	Fig.	Eq.	Fig.	Eq.	Fig.	Eq.	Fig.	Eq.	Fig.	Eq.	Fig.	Eq.	Eq.
$\phi_1$	B57	-----	B58	1	---	---	---	---	---	---	---	---	B59	---	---	---
$\phi_2$	---	-----	---	---	B57	---	B58	1	---	---	---	---	B59	---	---	---
$\beta'_1$ or $i$	B60	3(a)	B61	2(a)	---	---	---	---	B62	3(a)	---	---	B63	3(a)	---	---
$\beta'_2$ or $\delta$	---	-----	---	---	B60	3(a)	B61	2(a)	---	---	B62	3(a)	B63	3(a)	---	---
$\psi$	---	---	---	---	---	---	---	---	---	---	---	---	B64	---	B65	---
$\psi_i$	B66	-----	B67	---	B6 <sup>c</sup>	---	B69	---	B70	4(a)	B71	4(a)	B72	---	---	---
$\eta$	B73	-----	B73	---	B73	---	B73	---	B73	4(a)	B73	4(a)	B74	---	B75	---
$\bar{\omega}$	B76	2(a), 3(b)	B77	8(b)	B78	8(a)	B79	8(b)	B80	---	B81	---	B82	2(c)	B83	---
D	B84	6(a)	B85	9(a)	B86	9(b)	B87	9(c)	B88	---	B89	---	B90	2(c)	---	---
k	B91	2(a), 3(b)	B92	8(b)	---	---	---	---	B93	2(c)	---	---	---	---	---	B94

error calculations. Usually the equations are simpler if dimensionless terms such as  $(\Delta V_2/V_2)$  and  $[\Delta\eta/(1 - \eta)]$  are used. Some of the equations become much simpler when  $\beta_1$  is zero; when such is the case, the simplified form is included in the list of equations.

Carpet plots of some of the equations are presented in figures 1 to 9 to allow quick calculations. A carpet plot is simply a convenient way of showing a function of two variables. Each curve shown gives the relation between the function and one of the variables for a constant value of the other variable. For a function of more than two variables, a lattice arrangement of carpet plots can be used. Figure 6(a) is an example showing a function of four variables. The individual carpets are offset so that a french curve may be used for interpolation between plots. For many of the error equations, two plots are presented, one plot covering the range of conventional pump operation, the other covering the higher blade angles typical of inducer operation. Most of the error functions had considerably different values and/or slopes at high blade angles as compared with moderate blade angles, so a single plot would not be readable at both extremes.

Not all of the error equations are presented in plot form, since for simple linear relations this was deemed unnecessary. Some plots are used for more than one error equation but, to avoid confusion, only one equation is represented in the plot coordinates. Table I gives the equation numbers and figure numbers for the various combinations of performance parameters and design or measured variables. Some of the plotted values must be changed in sign or multiplied by a constant in order to correspond to a particular measurement equation; for this reason, one should always refer to the error equations first before using the plots.

The error equations were derived assuming small errors, but should be sufficiently accurate for most applications. An error equation gives the sensitivity to an error (i. e., the ratio of the change in a performance parameter to the change in a design or measured variable) at one particular set of conditions (i. e., for particular values of  $\beta'_1$ ,  $\beta'_2$ ,  $\varphi_2$ , etc.). A large error may change these conditions enough to significantly change the sensitivity. In this case, using the initial sensitivity to compute an error is not a good approximation. This possibility can be checked by comparing the sensitivity at two conditions differing by the amount of the assumed error.

## APPLICATION OF THE ERROR ANALYSIS

### Design Errors

The design error equations and carpet plots (figs. 1 to 9) relate the magnitude of

the errors in selected performance parameters to the amounts of errors in individual design variables. As an example, take the highly loaded rotor data discussed in appendix C, where at a radius ratio of 0.947 the measured values include  $\psi_1 = 0.391$ ,  $\beta_2 = 41.7^\circ$ , and  $\beta'_2 = 49.0^\circ$ . From figure 4(c), a  $1^\circ$  error in  $\beta'_2$  results in an error in  $\psi_1$  and  $\psi$  of -4.54 percent of the value of  $\psi_{12}$ . Since, for no prewhirl  $\psi_{12} = \psi_1$ , a  $1^\circ$  error in  $\beta'_2$  gives an error of -0.018 in  $\psi_1$  and  $\psi$ . Errors in  $\beta'_2$  can be caused either by design errors in deviation angle or by inaccuracies in the fabrication of the blade outlet angle. The errors shown by the other design error equations can be determined in a similar manner.

The error equations can be used to determine the sensitivity of a given hydrodynamic design to design errors and manufacturing tolerances. The ratio of a 0.018 error in  $\psi$  to a  $1^\circ$  error in  $\beta'_2$  may be regarded as a measure of the sensitivity of  $\psi$  to errors in  $\beta'_2$ . The sensitivity to errors may be important in comparing two competing designs. If it can be assumed that the size of the errors will not differ much in the designs being compared, the error equations will show which design is likely to meet its specifications the closest. It is not necessary to know the actual size of the errors in making this comparison.

In an iterative design procedure, the output values of one iteration are generally used to determine the input to the next iteration. A typical design procedure might have each iteration begin with new values of  $\bar{\omega}$ ,  $\delta$ , and  $r_2$ . Using the design error equations or plots, it can be determined whether the difference between the old and new values of these inputs are great enough to significantly affect the other parameters. Another approach is to terminate calculations when the differences between the new and old values of  $\bar{\omega}$  and  $\delta$  are less than the anticipated design errors. Comparing the new and old values of  $r_2$  is usually unnecessary. Values of  $r_2$  are generally determined from a radial equilibrium calculation in such a way that specifying  $\bar{\omega}$  and  $\delta$  will determine  $r_2$  for a given geometry. To summarize, the error equations can be used to set definite criteria on when to terminate the iterations.

In comparing design performance to measured performance, an error analysis may help determine the significance of any discrepancy. The question is whether an observed discrepancy is within the limits to be expected for a given error or combination of errors. The combined effect of errors in two or more design variables may be calculated using equation (2) or (3). A similar calculation may be made for measurement errors, or for a combination of design errors and measurement errors.

Estimates of uncertainty intervals in the performance parameters are obtained if the effects of random errors in all of the design variables are combined using equation (7). The uncertainty interval shows the range within which the parameter may be assumed to lie with reasonable probability. For example, a head-rise coefficient of 0.37 with an uncertainty interval of 0.02 for 90 percent probability means that there is

a 90 percent chance that the value of  $\psi$  is between 0.36 and 0.38. The uncertainty interval is the most reliable criterion of the accuracy of a set of data and is to be preferred in making such comparisons as design performance with measured performance. However, the uncertainty interval is dependent on estimates of errors in all of the design variables. If one or more of the error estimates are questionable, it may be better to restrict the comparisons to the design parameters with reasonably accurate error values.

## Measurement Errors

The measurement error equations and charts give the amount of error in selected performance parameters as functions of the amounts of measurement errors. One use of the measurement error analysis is to help in planning instrumentation. The error equations can be used to determine which measurement errors cause the greatest errors in the various performance parameters. Significant effort would be justified in order to improve the accuracy of a critical measurement, while only minimal effort should be applied to a measurement which introduces relatively small errors.

The effects of random errors due to different measurements may be combined using equation (3). If the errors due to all pertinent measurements are included, the result is an uncertainty interval in the measured performance parameter. Since it includes the effects of all known random errors, the uncertainty interval is the best criterion of normal data variability.

The measurement error calculation is useful in evaluating data trends. It gives an indication of the amount of data scatter which may reasonably be expected. If the scatter is small compared with the predicted amount of error, this indicates that the measurements are more consistent than anticipated. The error analysis may also show whether or not a change in the data is significant. For example, suppose that after a rotor is modified, the test data show a small increase in the values of blade element efficiency over the previous test data. It cannot be concluded that the modification improved the performance unless the differences are greater than can be explained by normal measurement errors. The amount of error to be expected is something to consider when evaluating any trend in a set of data.

The measurement error analysis is applied to two particular sets of test data in appendix C. The data chosen for this example (refs. 4 and 5) were for a highly loaded conventional rotor and for a flat-plate inducer. The results are presented in terms of uncertainty intervals. Many of the ideas discussed in a general way in this report are brought out in this example, among them the trends of sensitivity with blade angle and the use of the error analysis in choosing instrumentation. The example is intended to



show some of the results which can be obtained from the error analysis and some of the problems involved in its use and to give an idea of what degree of accuracy to expect in current pump test data.

## TRENDS SHOWN BY ERROR ANALYSIS

Using the carpet plots, some generalizations can be made on how the sensitivity to design and measurement errors will vary with different designs. The sensitivity of the performance parameters to design and measurement errors can be read directly from the curves of figures 1 to 9. The following paragraphs summarize the trends of sensitivity with changes in stagger angle and blade loading.

The effects of a change in stagger angle on the sensitivities to design and measurement errors are listed in table II. The table shows how the sensitivity of a particular performance parameter (shown in the column on the left) to errors in a given variable changes when stagger angle is increased. The intention of this table is to allow general trends with stagger angle to be visualized. So if a particular trend differs depending on the values of the flow angles, no attempt is made to show the trend under all possible design conditions. Rather, the trend under the most typical design condition is listed in the table, along with the restriction under which this trend applies.

For design errors, (table II(a)) the sensitivity trends show a strikingly regular pattern. The sensitivity of all of the pertinent performance parameters to errors in the outlet velocity diagram variables  $V_{Z2}$ ,  $\beta'_2$ , and  $r_2$  increase as stagger angle is increased. (The sensitivity of  $D$  to errors in  $r_2$  is a possible exception.) In contrast, the sensitivity to errors in the inlet velocity diagram variables  $V_{Z1}$  and  $\beta_1$  either decrease or do not change as stagger angle is increased. For typical pump designs, the sensitivity to errors in  $V_{Z2}$ ,  $\beta'_2$ , and  $r_2$  is considerably greater than the sensitivity to errors in  $V_{Z1}$  and  $\beta_1$ . Consequently, the total amount of error in the performance parameters follows the trend of the former variables.

The effects of a change in blade loading on the sensitivity to design errors were also determined. (These results are not included in table II.) The sensitivity of all of the performance parameters to errors in  $V_{Z2}$ ,  $\beta_2$ , and  $r_2$  decreases as loading is increased. As loading has no direct effect on the inlet velocity diagrams, the sensitivities to errors in  $V_{Z1}$  and  $\beta_1$  are not affected. The general conclusion is that the sensitivity to design errors in all of the performance parameters except  $V_1$  and  $\beta'_1$  tend to increase with increasing stagger angle or decreasing loading. For an inducer, the combination of high stagger angle and light loading make the design very susceptible to design errors.

The sensitivity of the measured performance parameters to measurement errors

TABLE II. - TRENDS OF SENSITIVITY TO ERRORS WITH INCREASING STAGGER ANGLE

## (a) Design errors

Performance parameter	Design variable					
	$V_{Z1}$	$\beta_1$	$V_{Z2}$	$\beta'_2$	$\bar{\omega}$	$r_2$
$V_1$	No change <sup>a</sup>	NCT <sup>b</sup>				
$\beta'_1$	Decreases (high blade angle) <sup>c</sup>	Decreases				
$V_2$			Increases (high blade angle)	Increases		Increases
$\beta_2$			Increases (except high $\beta_2$ )	Increases ( $\beta'_2 > \beta_2$ )		Increases (except high $\beta_2$ )
$\psi_i$	No change	NCT	Increases ( $\beta'_2 > \beta_2$ )	Increases (high blade angle)		Increases ( $\beta'_2 > \beta_2$ )
$\psi$	Decreases slightly (small $\beta_1$ )	Decreases slightly (small $\beta_1$ )	Increases ( $\beta'_2 > \beta_2$ )	Increases (high blade angle)	Decreases slightly	Increases ( $\beta'_2 > \beta_2$ )
$\eta$	Decreases (small $\beta_1$ )	NCT	Increases ( $\beta'_2 > \beta_2$ )	Increases (high blade angle)	No change	Increases ( $\beta'_2 > \beta_2$ )
D	Decreases (small $\beta_1$ )	Usually decreases (small $\beta_1$ )	Increases	Increases		NCT <sup>b</sup>

## (b) Measurement errors

Performance parameter	Measured variables							
	$V_1$	$\beta_1$	$V_2$	$\beta_2$	$r_1$	$r_2$	$U_t$	$\Delta H$
$\varphi_2$			No change <sup>a</sup>	Increases			No change	
$\beta'_2$			Decreases (high blade angle) <sup>c</sup>	Increases (high blade angle)		NCT <sup>b</sup>	Decreases (high blade angle)	
$\psi$							No change	No change
$\psi_i$	No change	Decreases	No change	Decreases	NCT	NCT	No change	
$\eta$	No change	Decreases	No change	Decreases	NCT	NCT	No change	No change
$\bar{\omega}$	Usually decreases	Decreases (high blade angle)	Usually increases	Decreases (high blade angle)	NCT	NCT	NCT	Slight increase
D	Usually decreases	Usually decreases	Increases (high blade angle)	Usually decreases	NCT	NCT	Increases	

<sup>a</sup>Stagger angle does not change the sensitivity.<sup>b</sup>No consistent trend of sensitivity with stagger angle.<sup>c</sup>Parenteticals show conditions under which the trend applies. The restriction to high blade angles is never more severe than  $\beta'_1 > 45^\circ$  or  $\beta_2 + \beta'_2 > 90^\circ$ .

is also affected by changes in stagger angle and blade loading. However, unlike the design error case, the sensitivity trends of the measurement errors showed no regular pattern. The individual trends with stagger angle are listed in table II(b). For increases in blade loading, the sensitivity to errors either increases or does not change for all of the measurement error equations. The overall level of measurement errors (due to all sources of error), as compared with design errors, will in general be less affected by changes in stagger angle or blade loading.

Some of the sensitivity trends are not immediately obvious from the carpet plots. For example, the sensitivity of  $\psi_i$  to design errors in  $\beta'_2$  (fig. 4(c)) increases with increasing  $\beta'_2$ , but decreases with increasing  $\beta_2$ . The trend with stagger angle will depend on which effect is stronger. In preparing table II, sample calculations were made for each case in which the trends in  $\beta_2$  and  $\beta'_2$  were opposed. It was found that whenever  $\beta'_2$  was greater than  $\beta_2$ , the trend with  $\beta'_2$  predominated. For most blade elements in a conventional pump design,  $\beta'_2$  is greater than  $\beta_2$ ; consequently, the trend with  $\beta'_2$  determines the trend of sensitivity with stagger angle for most blade elements.

## Application of Error Equations to Stators

The design equations and measurement equations for stators differ from the related rotor equations in that, since  $U_s = 0$ , there is no distinction between relative and absolute velocities, and  $\psi_i$  is zero. The stator error equations, which are derived from the stator design and measurement equations, also differ from the related rotor error equations. The two sets of error equations are, however, enough alike so that a few substitutions will produce the stator error equations from the rotor error equations. Therefore, even though the error equations presented herein were developed for rotors, they can, with suitable modifications, be applied to stators.

The error equations for stators can be obtained from the listed error equations by making the following substitutions:

- (1) Whenever a relative angle appears, substitute the negative of the absolute angle; that is, substitute  $-\beta_{1s}$  for  $\beta'_1$ ,  $-\beta_{2s}$  for  $\beta'_2$ , and  $-\Delta\beta_{2s}$  for  $\Delta\beta'_2$ .
- (2) For  $\psi_i$ , substitute 0.
- (3) For all other parameters, substitute the corresponding stator parameter.
- (4) In the error equations for  $D$ , change the sign of the second term (the term continuing  $\sigma$ ). This is required because, in the definition of  $D = 1 - \frac{V_2}{V_1} + \frac{\Delta V_\theta}{2\sigma V_1}$ , the turning ( $\Delta V_\theta$  term) is in the opposite direction for a stator than for a rotor.
- (5) These substitutions give the correct stator error equation with one exception,

equation (B42). The sign on the whole equation (not just the second term) should be changed and  $(r_2 V_{\theta 2} - r_1 V_{\theta 1})/V_{Z2} r_t$  substituted for  $\psi_i/\varphi_2$ .

After these substitutions are made, the resulting equation may simplify. For example, equation (B15) becomes

$$\begin{aligned} \left( \frac{\Delta V_{2s}}{V_{2s}} \right) &= -\cos^2 \beta_{2s} \left( -\tan^2 \beta_{2s} - 1 \right) \frac{\Delta V_{Z2s}}{V_{Z2s}} \\ &= \cos^2 \beta_{2s} \sec^2 \beta_{2s} \frac{\Delta V_{Z2s}}{V_{Z2s}} = \frac{\Delta V_{Z2s}}{V_{Z2s}} \end{aligned}$$

The error equations for the performance parameters  $\psi_i$ ,  $\eta$ ,  $\beta'_1$ , and  $\beta'_2$  become either meaningless or trivial when applied to stators and would not be included in a stator error analysis. For stators,  $\eta$  is not defined,  $\psi_i$  is identically zero, and  $\beta'_1$  and  $\beta'_2$  are the same as  $\beta_1$  and  $\beta_2$  which are input variables in the stator error equations. However, the error equations in which  $\beta'_2$  appears as a design variable should not be dropped from the analysis. Using the substitutions, these equations are transformed into stator error equations in  $\beta_2$  which are necessary for a complete error analysis.

The stator counterpart of head-rise coefficient  $\psi_s$  can be defined using the value of  $U_t$  from the preceeding rotor. The error equations derived for  $\psi_s$  will then give the effect of stator errors on the stage head-rise coefficient.

For stators, the design and measurement equations for the inlet parameters  $V_{1s}$  and  $\varphi_{1s}$  are identical in form to those for the outlet parameters  $V_{2s}$  and  $\varphi_{2s}$ . As would be expected, the derived error equations show the same similarity. The inlet error equations are easier to derive and can then be applied to both inlet and outlet parameters.

## CONCLUDING REMARKS

The basic purpose of this report is to provide a method for calculating the effects of design errors and measurement errors on pump performance. Error equations were developed which allow the amount of error in a given performance parameter to be calculated from the amount of error in a given design or measured variable. These error equations apply essentially to flow along streamlines or along individual blade elements. The errors due to more than one source can often be combined and treated as a unit.

For random errors, the uncertainty interval is used to indicate the combined effect of a number of errors on a given performance parameter.

A number of uses of the error analysis procedures are pointed out in this report. The error analysis is most often used to determine the accuracy of the performance parameter values as an aid in interpreting design or measured data. The error analysis is also used to determine the critical measurement, or critical step in a design procedure, which introduces the greatest amount of error.

The sensitivity of most of the performance parameters to design errors increased with increasing stagger angle or decreasing loading. Inducers, which have a combination of high stagger angle and light loading, are especially susceptible to design errors. No regular pattern was noted in the trends of the sensitivity to measurement errors with changes in stagger angle and loading.

The error equations, as written, apply to rotors. Modifications which allow them to be applied to stators were pointed out.

A limitation of an error analysis of this type is that it depends on estimates of the magnitudes of design errors or measurement errors. The calculated values of errors in the performance parameters are only as accurate as the input error estimates.

For pump rotor test measurements, reasonably good estimates can usually be made of the inherent accuracies of instrumentation such as pressure transducers and data recording equipment. However, errors due to probe responses to pressure fluctuations, flow fluctuations, and radial pressure gradients are difficult to evaluate. If a single probe measurement is used, circumferential variations in pressures and velocities are not accounted for. There is also the question of how well a stationary probe measurement will average out the blade-to-blade variations in pressures and flow angles.

In a design procedure, it is difficult to assess the accuracy of certain inputs, notably loss coefficient and deviation angle. Accuracy estimates are generally obtained from correlations of previous test data, but the amount of suitable axial flow pump data is rather limited. It is also difficult to estimate the accuracy of the outlet axial velocity, but for a different reason. In a design system, the outlet axial velocity is calculated from the requirements of radial equilibrium and continuity. This means that the error in outlet velocity at a given blade element will be affected by the errors at other blade elements.

The error equations were derived primarily for axial flow pumps, but are not limited to axial flow. All of the design error equations and measurement error equations are correct for mixed flow impellers and centrifugal pumps if the meridional velocity is substituted for axial velocity. However, the error equations apply to a design

system and test procedures which are standard for axial flow pumps, but are not always used for mixed-flow impellers.

Lewis Research Center,  
National Aeronautics and Space Administration,  
Cleveland, Ohio, January 20, 1970,  
128-31.

## APPENDIX A

### SYMBOLS

D	diffusion factor	$\eta$	blade element efficiency
f	general performance parameter	$\varphi$	flow coefficient
g	gravitational acceleration constant	$\sigma$	solidity
H	total head, ft; m	$\psi$	head rise coefficient
$\Delta H$	head rise, ft; m	$\bar{\omega}$	total-pressure loss coefficient
$H_{sv}$	net positive suction head, ft; m	Subscripts:	
i	incidence angle, deg	i	ideal
k	cavitation number	m, n	dummy variables
r	radius, ft; m	s	stator
U	rotor speed, ft/sec; m/sec	t	tip
V	fluid velocity, ft/sec; m/sec	Z	axial direction
x	general design or measured variable	$\theta$	tangential direction
$\beta$	fluid angle, angle between fluid velocity and axial direction, deg	1	rotor inlet
$\Delta$	uncertainty interval or finite difference	2	rotor outlet
$\delta$	deviation angle, deg	Superscripts:	
		'	relative to rotor

## APPENDIX B

### ERROR ANALYSIS EQUATIONS

The equations derived for the error analysis are identified by "des" or "meas," showing either a design error equation or a measurement error equation, respectively; followed by symbols showing the parameters involved. Thus des -  $V_2:V_{Z2}$  identifies the design error equation giving the error in the performance parameter  $V_2$  for a unit error in the design variable  $V_{Z2}$ . The error equations are also identified by number, with table I giving the equation number corresponding to each possible combination of performance parameter and design or measured variable. Table I also gives the figure numbers of the carpet plots corresponding to the equations. The table is complete for all of the listed performance parameters and design variables or measured variables, so the omission of a possible combination of variables means that the performance parameter involved is not a function of the input design or measured variable.

#### Design Equations

The design-error equations were derived from the following equations:

$$V_1 = V_{Z1} \sec \beta_1 \quad (B1)$$

$$V_{\theta 1} = V_{Z1} \tan \beta_1 \quad (B2)$$

$$(V'_1)^2 = V_{Z1}^2 + (U_1 - V_{Z1} \tan \beta_1)^2 \quad (B3)$$

$$\beta'_1 = \tan^{-1} \left( \frac{U_1}{V_{Z1}} - \tan \beta_1 \right) \quad (B4)$$

$$V'_2 = V_{Z2} \sec \beta'_2 \quad (B5)$$

$$\beta_2 = \tan^{-1} \left( \frac{U_2}{V_{Z2}} - \tan \beta'_2 \right) \quad (B6)$$



$$V_{\theta 2} = U_2 - V_{Z2} \tan \beta_2' \quad (B7)$$

$$V_2^2 = V_{Z2}^2 + (U_2 - V_{Z2} \tan \beta_2')^2 \quad (B8)$$

$$\psi_i = \frac{1}{U_T^2} (U_2 V_{\theta 2} - U_1 V_{\theta 1}) \quad (B9)$$

$$\psi = \psi_i - \frac{1}{2} \frac{\overline{\omega}(V_1')^2}{U_t^2} \quad (B10)$$

$$\eta = \frac{\psi}{\psi_i} \quad (B11)$$

$$D = 1 - \frac{V_2'}{V_1'} + \frac{r_2 V_{\theta 2} - r_1 V_{\theta 1}}{\sigma V_1' (r_1 + r_2)} \quad (B12)$$

### Design-Error Equations

The resulting differential formulas are the following:

des -  $V_1:V_{Z1}$

$$\left( \frac{\Delta V_1}{V_1} \right) = \left( \frac{\Delta V_{Z1}}{V_{Z1}} \right) \quad (B13)$$

des -  $V_1:\beta_1$  (fig. 1)

$$\left( \frac{\Delta V_1}{V_1} \right) = \frac{\pi}{180} \tan \beta_1 \Delta \beta_1 \quad (B14)$$

des -  $V_2:V_{Z2}$  (fig. 2(a))

$$\left( \frac{\Delta V_2}{V_2} \right) = - \cos^2 \beta_2 (\tan \beta_2' \tan \beta_2 - 1) \frac{\Delta V_{Z2}}{V_{Z2}} \quad (B15)$$

des -  $V_2:\beta_2'$  (fig. 2(b))

$$\left(\frac{\Delta V_2}{V_2}\right) = -\frac{\pi}{180} \sin \beta_2 \cos \beta_2 \sec^2 \beta_2' \Delta \beta_2' \quad (B16)$$

des -  $V_2:r_2$  (fig. 2(c))

$$\left(\frac{\Delta V_2}{V_2}\right) = \sin \beta_2 \cos \beta_2 (\tan \beta_2' + \tan \beta_2) \frac{\Delta r_2}{r_2} \quad (B17)$$

des -  $\beta_1':V_{Z1}$  (fig. 3(a))

$$\Delta \beta_1' = -\frac{180}{\pi} \cos^2 \beta_1' (\tan \beta_1' + \tan \beta_1) \frac{\Delta V_{Z1}}{V_{Z1}} \quad (B18)$$

des -  $\beta_1':\beta_1$  (fig. 3(b))

$$\Delta \beta_1' = -\cos^2 \beta_1' \sec^2 \beta_1 \Delta \beta_1 \quad (B19)$$

des -  $\beta_2':V_{Z2}$  (In fig. 3(a) substitute  $\beta_2$  for  $\beta_1'$  and  $\beta_2'$  for  $\beta_1$ .)

$$\Delta \beta_2' = -\frac{180}{\pi} \cos^2 \beta_2' (\tan \beta_2' + \tan \beta_2) \frac{\Delta V_{Z2}}{V_{Z2}} \quad (B20)$$

des -  $\beta_2:\beta_2'$  (In fig. 3(b) substitute  $\beta_2$  for  $\beta_1'$  and  $\beta_2'$  for  $\beta_1$ .)

$$\Delta \beta_2 = -\cos^2 \beta_2 \sec^2 \beta_2' \Delta \beta_2' \quad (B21)$$

des -  $\beta_2:r_2$  (In fig. 3(a) substitute  $\beta_2$  for  $\beta_1'$  and  $\beta_2'$  for  $\beta_1$ ; multiply result by -1.)

$$\Delta \beta_2 = \frac{180}{\pi} \cos^2 \beta_2 (\tan \beta_2' + \tan \beta_2) \frac{\Delta r_2}{r_2} \quad (B22)$$

des -  $\psi_i:V_{Z1}$

$$\left(\frac{\Delta\psi_i}{\psi_{i1}}\right) = -\frac{\Delta V_{Z1}}{V_{Z1}} \quad (\text{B23})$$

where

$$\psi_{i1} = \frac{U_1 V_{\theta 1}}{U_t^2} = \frac{r_1}{r_t} \varphi_1 \tan \beta_1 \quad (\text{B24})$$

$$\psi_{i1} = 0 \quad \text{for } \beta_1 = 0$$

des -  $\psi_i:\beta_1$  (fig. 4(a))

$$\left(\frac{\Delta\psi_i}{\psi_{i1}}\right) = -\frac{\pi}{180} \sec \beta_1 \csc \beta_1 \Delta\beta_1 \quad (\text{B25})$$

In figure 4(a), the answer given is not a percent error in  $\psi_i$ , but the error in  $\psi_i$  is given as a percentage of  $\psi_{i1}$ , corresponding to the form of equation (B25). Similarly, figures 4(b) to (d) give errors in  $\psi_i$  as percentages of  $\psi_{i2}$ .

des -  $\psi_i:V_{Z2}$  (fig. 4(b))

$$\left(\frac{\Delta\psi_i}{\psi_{i2}}\right) = -\tan \beta_2' \cot \beta_2 \frac{\Delta V_{Z2}}{V_{Z2}} \quad (\text{B26})$$

where

$$\psi_{i2} = \frac{U_2 V_{\theta 2}}{U_t^2} = \frac{r_2}{r_t} \varphi_2 \tan \beta_2 \quad (\text{B27})$$

$$\psi_{i2} = \psi_i \quad \text{for } \beta_1 = 0$$

des -  $\psi_i:\beta_2'$  (fig. 4(c))

$$\left(\frac{\Delta\psi_i}{\psi_{i2}}\right) = -\frac{\pi}{180} \sec^2 \beta'_2 \cot \beta_2 \Delta\beta'_2 \quad (\text{B28})$$

des -  $\psi_i:r_2$  (fig. 4(d))

$$\left(\frac{\Delta\psi_i}{\psi_{i2}}\right) = (2 + \tan \beta'_2 \cot \beta_2) \frac{\Delta r_2}{r_2} \quad (\text{B29})$$

des -  $\psi:V_{Z1}$  (Multiply values from fig. 5(a) by  $\bar{\omega}\varphi_1^2$ . The  $\Delta\psi_i$  term is obtained from eq. (B23).)

$$\Delta\psi = \Delta\psi_i + \bar{\omega}\varphi_1^2(\tan \beta'_1 \tan \beta_1 - 1) \frac{\Delta V_{Z1}}{V_{Z1}} \quad (\text{B30})$$

$$\Delta\psi = -\bar{\omega}\varphi_1^2 \frac{\Delta V_{Z1}}{V_{Z1}} \quad \text{for } \beta_1 = 0$$

des -  $\psi:\beta_1$  (Multiply value from fig. 5(b) by  $\bar{\omega}\varphi_1^2$ ; use eq. (B25) for  $\Delta\psi_i$ .)

$$\Delta\psi = \Delta\psi_i + \frac{\pi}{180} \bar{\omega}\varphi_1^2 \tan \beta'_1 \sec^2 \beta_1 \Delta\beta_1 \quad (\text{B31})$$

des -  $\psi:V_{Z2}, \beta'_2, r_2$  (see eqs. (B26), (B28), and (B29))

$$\Delta\psi = \Delta\psi_i \quad (\text{B32})$$

des -  $\psi:\bar{\omega}$

$$\Delta\psi = -\frac{1}{2} \varphi_1^2 \sec^2 \beta'_1 \Delta\bar{\omega} \quad (\text{B33})$$

des -  $\eta:V_{Z1}$  (In fig. 2(a) substitute  $\beta'_1$  for  $\beta_2$  and  $\beta_1$  for  $\beta'_2$ , and multiply result by -2; use eq. (B23) for  $\Delta\psi_i$ . Answer is error in  $\eta$  as percent of  $1 - \eta$ .)

$$\left(\frac{\Delta\eta}{1 - \eta}\right) = \frac{1}{\psi_i} \Delta\psi_i + 2 \cos^2 \beta'_1 (\tan \beta'_1 \tan \beta_1 - 1) \frac{\Delta V_{Z1}}{V_{Z1}} \quad (\text{B34})$$

des -  $\eta:\beta_1$  (In fig. 2(b) substitute  $\beta_1'$  for  $\beta_2$  and  $\beta_1$  for  $\beta_2'$ , multiply result by -2;  
use eq. (B25) for  $\Delta\psi_i$ .)

$$\left(\frac{\Delta\eta}{1-\eta}\right) = \frac{1}{\psi_i} \Delta\psi_i + \frac{\pi}{90} \sin \beta_1' \cos \beta_1' \sec^2 \beta_1 \Delta\beta_1 \quad (\text{B35})$$

des -  $\eta:V_{Z2}, \beta_2', r_2$  (see eqs. (B26), (B28), and (B29))

$$\left(\frac{\Delta\eta}{1-\eta}\right) = \frac{1}{\psi_i} \Delta\psi_i \quad (\text{B36})$$

des -  $\eta:\bar{\omega}$

$$\left(\frac{\Delta\eta}{1-\eta}\right) = -\frac{\Delta\bar{\omega}}{\bar{\omega}} \quad (\text{B37})$$

In equations (B38) and (B39) use  $\sigma(r_1 + r_2)/2r_1$  in place of  $\sigma$  if  $r_2$  does not equal  $r_1$ .

des -  $D:V_{Z1}$  (see fig. 6(a))

$$\Delta D = -\left[(1-D)\cos^2\beta_1'(\tan\beta_1' \tan\beta_1 - 1) + \frac{1}{2\sigma} \tan\beta_1 \cos\beta_1'\right] \frac{\Delta V_{Z1}}{V_{Z1}} \quad (\text{B38})$$

$$\Delta D = (1-D)\cos^2\beta_1' \frac{\Delta V_{Z1}}{V_{Z1}} \quad \text{for } \beta_1 = 0$$

des -  $D:\beta_1$  (see fig. 6(b))

$$\Delta D = -\frac{\pi}{180} \left[(1-D)\sin\beta_1' \cos\beta_1' \sec^2\beta_1 + \frac{1}{2\sigma} \sec^2\beta_1 \cos\beta_1'\right] \Delta\beta_1 \quad (\text{B39})$$

In equations (B40) to (B45) use  $\sigma(r_1 + r_2)/2r_2$  in place of  $\sigma$  if  $r_2$  does not equal  $r_1$ .

des -  $D:V_{Z2}$  (see fig. 6(c))

$$\frac{V_1'}{V_2'} \Delta D = -\left(1 + \frac{\sin\beta_2'}{2\sigma}\right) \frac{\Delta V_{Z2}}{V_{Z2}} \quad (\text{B40})$$

des - D: $\beta'_2$  (see fig. 6(d))

$$\frac{V'_2}{V'_1} \Delta D = - \frac{\pi}{180} \left( \tan \beta'_2 + \frac{\sec \beta'_2}{2\sigma} \right) \Delta \beta'_2 \quad (\text{B41})$$

des - D: $r_2$

$$\begin{aligned} \frac{V'_1}{V'_2} \Delta D &= \frac{\cos \beta'_2}{2\sigma} \left( 2 \tan \beta_2 + \tan \beta'_2 - \frac{r_t}{r_1 + r_2} \frac{\psi_i}{\varphi_2} \right) \frac{\Delta r_2}{r_2} \\ &= M \left( N - \frac{r_t}{r_1 + r_2} \frac{\psi_i}{\varphi_2} \right) \frac{\Delta r_2}{r_2} \end{aligned} \quad (\text{B42})$$

where (see figs. 7(a) and (b))

$$M = \frac{\cos \beta'_2}{2\sigma} \quad (\text{B43})$$

$$N = 2 \tan \beta_2 + \tan \beta'_2 \quad (\text{B44})$$

An alternate form for  $\beta_1 = 0$  is

$$\frac{V'_1}{V'_2} \Delta D = \frac{\cos \beta'_2}{2\sigma} \left[ \left( 2 - \frac{r_2}{r_1 + r_2} \right) \tan \beta_2 + \tan \beta'_2 \right] \frac{\Delta r_2}{r_2} \quad (\text{B45})$$

## Measurement Equations

The measurement-error equations were derived from the following equations. Where similar equations apply to corresponding inlet and outlet parameters (such as  $V_{Z1}$  and  $V_{Z2}$ ), the subscript 1 or 2 is omitted.

$$V_Z = V \cos \beta \quad (\text{B46})$$

$$V_\theta = V \sin \beta \quad (\text{B47})$$

$$\varphi = \frac{V_Z}{U_t} \quad (B48)$$

$$V'^2 = V_Z^2 + (U - V_\theta)^2 \quad (B49)$$

$$\beta' = \tan^{-1} \left( \frac{U}{V_Z} - \tan \beta \right) \quad (B50)$$

$$\psi_i = \frac{1}{U_t^2} (U_2 V_{\theta 2} - U_1 V_{\theta 1}) \quad (B51)$$

$$\psi = \frac{g \Delta H}{U_t^2} \quad (B52)$$

$$\eta = \frac{\psi}{\psi_i} \quad (B53)$$

$$\bar{\omega} = \frac{2(\psi_i - \psi) U_t^2}{(V'_1)^2} \quad (B54)$$

$$D = 1 - \frac{V'_2}{V'_1} + \frac{r_2 V_{\theta 2} - r_1 V_{\theta 1}}{\sigma V'_1 (r_1 + r_2)} \quad (B55)$$

$$k = \frac{2gH_{sv} - V_1^2}{(V'_1)^2} \quad (B56)$$

## Measurement Error Equations

The resulting differential formulas are

$$\text{meas} - \varphi_{1,2} V_{1,2}$$

$$\frac{\Delta\varphi}{\varphi} = \frac{\Delta V}{V} \quad (\text{B57})$$

meas -  $\varphi_{1,2}:\beta_{1,2}$  (In fig. 1 multiply result by -1.)

$$\left(\frac{\Delta\varphi}{\varphi}\right) = -\frac{\pi}{180} \tan \beta \Delta\beta \quad (\text{B58})$$

meas -  $\varphi_{1,2}:U_t$

$$\left(\frac{\Delta\varphi}{\varphi}\right) = -\frac{\Delta U_t}{U_t} \quad (\text{B59})$$

meas -  $\beta'_{1,2}:V_{1,2}$  (fig. 3(a))

$$\Delta\beta' = -\frac{180}{\pi} \cos^2\beta'(\tan\beta' + \tan\beta) \frac{\Delta V}{V} \quad (\text{B60})$$

meas -  $\beta'_{1,2}:\beta_{1,2}$  (In fig. 2(a) substitute  $\beta'$  for  $\beta_2$  and  $\beta$  for  $\beta'_2$ ; multiply result by -1.)

$$\Delta\beta' = \cos^2\beta'(\tan\beta' \tan\beta - 1)\Delta\beta \quad (\text{B61})$$

meas -  $\beta'_{1,2}:r_{1,2}$  (In fig. 3(a)) multiply by -1; subtract  $r(d\beta'/dr)$  where  $d\beta'/dr$  is determined graphically.)

$$\Delta\beta' = -\left[r \frac{d\beta'}{dr} - \frac{180}{\pi} \cos^2\beta'(\tan\beta' + \tan\beta)\right] \frac{\Delta r}{r} \quad (\text{B62})$$

meas -  $\beta'_{1,2}:U_t$  (In fig. 3(a) multiply result by -1.)

$$\Delta\beta' = \frac{180}{\pi} \cos^2\beta'(\tan\beta' + \tan\beta) \frac{\Delta U_t}{U_t} \quad (\text{B63})$$

meas -  $\psi:U_t$

$$\left(\frac{\Delta\psi}{\psi}\right) = -2 \frac{\Delta U_t}{U_t} \quad (\text{B64})$$



meas -  $\psi:\Delta H$

$$\left(\frac{\Delta\psi}{\psi}\right) = \frac{\Delta(\Delta H)}{\Delta H} \quad (\text{B65})$$

In the following equations,  $\psi_{i1}$  and  $\psi_{i2}$  are as defined in equations (B24) and (B27).

meas -  $\psi_i:V_1$

$$\left(\frac{\Delta\psi_i}{\psi_{i1}}\right) = -\frac{\Delta V_1}{V_1} \quad (\text{B66})$$

meas -  $\psi_i:\beta_1$

$$\Delta\psi_i = -\frac{\pi}{180} \frac{r_1}{r_t} \varphi_1 \Delta\beta_1 \quad (\text{B67})$$

meas -  $\psi_i:V_2$

$$\left(\frac{\Delta\psi_i}{\psi_{i2}}\right) = \frac{\Delta V_2}{V_2} \quad (\text{B68})$$

meas -  $\psi_i:\beta_2$

$$\Delta\psi_i = \frac{\pi}{180} \frac{r_2}{r_t} \varphi_2 \Delta\beta_2 \quad (\text{B69})$$

meas -  $\psi_i:r_1$  (In fig. 4(a) multiply result by  $-\text{d}\beta_1/\text{d}r_1$ ; add  $(1/\varphi_1)(\text{d}\varphi_1/\text{d}r_1)$ .)

$$\Delta\psi_i = \psi_{i1} \left( \frac{1}{\varphi_1} \frac{\text{d}\varphi_1}{\text{d}r_1} + \frac{\pi}{180} \sec \beta_1 \csc \beta_1 \frac{\text{d}\beta_1}{\text{d}r_1} \right) \Delta r_1 \quad (\text{B70})$$

This expression is indeterminate for a  $\beta_1$  of 0. If  $\beta_1 = 0$ ,

$$\Delta\psi_i = \frac{\pi}{180} \frac{r_1}{r_t} \varphi_1 \frac{\text{d}\beta_1}{\text{d}r_1} \Delta r_1$$

meas -  $\psi_i:r_2$  (In fig. 4(a) substitute  $\beta_2$  for  $\beta_1$ , multiply result by  $d\beta_2/dr_2$  and subtract  $(1/\varphi_2)(d\varphi_2/dr_2)$ .)

$$\Delta\psi_i = -\psi_i \left( \frac{1}{\varphi_2} \frac{d\varphi_2}{dr_2} + \frac{\pi}{180} \sec \beta_2 \csc \beta_2 \frac{d\beta_2}{dr_2} \right) \Delta r_2 \quad (\text{B71})$$

$$\Delta\psi_i = - \left( \frac{d\psi_i}{dr_2} - \frac{\psi_i}{r_2} \right) \Delta r_2 \quad \text{for } \beta_1 = 0$$

meas -  $\psi_i:U_t$

$$\Delta\psi_i = -\psi_i \frac{\Delta U_t}{U_t} \quad (\text{B72})$$

meas -  $\eta:V_1, \beta_1, V_2, \beta_2, r_1, r_2$

$$\left( \frac{\Delta\eta}{\eta} \right) = - \frac{1}{\psi_i} \Delta\psi_i \quad (\text{B73})$$

meas -  $\eta:U_t$

$$\left( \frac{\Delta\eta}{\eta} \right) = - \frac{\Delta U_t}{U_t} \quad (\text{B74})$$

meas -  $\eta:\Delta H$

$$\left( \frac{\Delta\eta}{\eta} \right) = \frac{\Delta(\Delta H)}{\Delta H} \quad (\text{B75})$$

meas -  $\bar{\omega}:V_1$  (In fig. 2(a) substitute  $\beta'_1$  for  $\beta_2$ ,  $\beta_1$  for  $\beta'_2$ , multiply result by  $2(1 - \bar{\omega})$ , and add 2 times fig. 3(b).)

$$\Delta\bar{\omega} = -2 \cos^2 \beta'_1 \left[ (1 - \bar{\omega})(\tan \beta'_1 \tan \beta_1 - 1) + \sec^2 \beta_1 \right] \frac{\Delta V_1}{V_1} \quad (\text{B76})$$

$$\Delta\bar{\omega} = -2\bar{\omega} \cos^2 \beta'_1 \frac{\Delta V_1}{V_1} \quad \text{for } \beta_1 = 0$$

meas -  $\bar{\omega}:\beta_1$  (In fig. 8(b) substitute  $\beta_1'$  for  $\beta_2'$  and  $\beta_1$  for  $\beta_2$ ; multiply result by  $-(1 - \bar{\omega})$ .)

$$\Delta\bar{\omega} = -\frac{\pi}{90} (1 - \bar{\omega}) \cos^2 \beta_1' (\tan \beta_1' + \tan \beta_1) \Delta\beta_1 \quad (\text{B77})$$

meas -  $\bar{\omega}:V_2$  (fig. 8(a))

$$\frac{V_1'^2}{V_2'^2} \Delta\bar{\omega} = 2 \cos^2 \beta_2' \left[ (\tan \beta_2' \tan \beta_2 - 1) + \sec^2 \beta_2' \right] \frac{\Delta V_2}{V_2} \quad (\text{B78})$$

meas -  $\bar{\omega}:\beta_2$  (fig. 8(b))

$$\frac{V_1'^2}{V_2'^2} \Delta\bar{\omega} = \frac{\pi}{90} \cos^2 \beta_2' (\tan \beta_2' + \tan \beta_2) \Delta\beta_2 \quad (\text{B79})$$

meas -  $\bar{\omega}:r_1$  (see eqs. (B76) and (B77))

$$\Delta\bar{\omega} = - \left[ \left( \frac{\Delta\bar{\omega}}{\Delta V_1} \right) \frac{dV_1}{dr_1} + \left( \frac{\Delta\bar{\omega}}{\Delta \beta_1} \right) \frac{d\beta_1}{dr_1} + \frac{2g}{V_1'^2} \frac{dH_{sv}}{dr_1} \right] \Delta r_1 \quad (\text{B80})$$

$$\Delta\bar{\omega} = 0 \quad \text{for constant } V_1, H_{sv}, \text{ and } \beta_1 \text{ (usually } \beta_1 = 0)$$

meas -  $\bar{\omega}:r_2$

$$\Delta\bar{\omega} = 2 \frac{\cos^2 \beta_1'}{\varphi_1^2} \left( \frac{\psi_{i2}}{r_2} - \frac{d\psi_{i2}}{dr_2} + \frac{d\psi}{dr_2} \right) \Delta r_2 \quad (\text{B81})$$

$$\Delta\bar{\omega} = \frac{2}{\left( \frac{r_1}{r_t} \right)^2 + \varphi_1^2} \left( \frac{\psi_i}{r_2} - \frac{d\psi_i}{dr_2} + \frac{d\psi}{dr_2} \right) \Delta r_2 \quad \text{for } \beta_1 = 0 \text{ and constant } H_{sv}$$

The term  $d\psi/dr_2$  denotes a change in  $\psi$  produced by a change in only the outlet probe radius, that is,  $g/U_t^2(dH_2/dr_2)$  rather than  $g/U_t^2(d\Delta H/dr_2)$ . However, the radial variations in  $H_1$  are usually small compared with those in  $H_2$ , in which case the second form can be used.

meas -  $\bar{\omega}:U_t$  (In fig. 2(c) substitute  $\beta'_1$  for  $\beta_2$ ,  $\beta_1$  for  $\beta'_2$ , multiply result by  $-2\bar{\omega}$ , and add  $2 \cos^2 \beta'_1 \psi_i / \varphi_1^2$ .)

$$\Delta \bar{\omega} = \left[ -2\bar{\omega} \sin \beta'_1 \cos \beta'_1 (\tan \beta'_1 + \tan \beta_1) + 2 \cos^2 \beta'_1 \frac{\psi_i}{\varphi_1^2} \right] \frac{\Delta U_t}{U_t} \quad (B82)$$

$$\Delta \bar{\omega} = \left[ -2\bar{\omega} \sin^2 \beta'_1 + 2 \cos^2 \beta'_1 \frac{\psi_i}{\varphi_1^2} \right] \frac{\Delta U_t}{U_t} \quad \text{for } \beta_1 = 0$$

meas -  $\bar{\omega}:\Delta H$

$$\Delta \bar{\omega} = - \frac{2g}{V_1'^2} \Delta(\Delta H) \quad (B83)$$

In equations (B84) and (B85) use  $\sigma(r_1 + r_2)/2r_1$  in place of  $\sigma$  if  $r_2$  does not equal  $r_1$ .

meas -  $D:V_1$  (fig. 6(a))

$$\Delta D = - \left[ (1 - D) \cos^2 \beta'_1 (\tan \beta'_1 \tan \beta_1 - 1) + \frac{1}{2\sigma} \cos \beta'_1 \tan \beta_1 \right] \frac{\Delta V_1}{V_1} \quad (B84)$$

$$\Delta D = (1 - D) \cos^2 \beta'_1 \frac{\Delta V_1}{V_1} \quad \text{for } \beta_1 = 0$$

meas -  $D:\beta_1$  (fig. 9(a))

$$\Delta D = - \frac{\pi}{180} \left[ (1 - D) \cos^2 \beta'_1 (\tan \beta'_1 + \tan \beta_1) + \frac{1}{2\sigma} \cos \beta'_1 \right] \Delta \beta_1 \quad (B85)$$

In equations (B86) and (B87), use  $[\sigma(r_1 + r_2)]/2r_2$  in place of  $\sigma$  if  $r_2$  does not equal  $r_1$ .

meas - D:V<sub>2</sub> (fig. 9(b))

$$\frac{V'_1}{V'_2} \Delta D = \left[ \cos^2 \beta'_2 (\tan \beta'_2 \tan \beta_2 - 1) + \frac{1}{2\sigma} \tan \beta_2 \cos \beta'_2 \right] \frac{\Delta V_2}{V_2} \quad (\text{B86})$$

meas - D:β<sub>2</sub> (fig. 9(c))

$$\frac{V'_1}{V'_2} \Delta D = \frac{\pi}{180} \left[ \cos^2 \beta'_2 (\tan \beta'_2 + \tan \beta_2) + \frac{1}{2\sigma} \cos \beta'_2 \right] \Delta \beta_2 \quad (\text{B87})$$

meas - D:r<sub>1</sub> (see eqs. (B84) and (B85))

$$\Delta D = - \left[ \left( \frac{\Delta D}{\Delta V_1} \right) \frac{dV_1}{dr_1} + \left( \frac{\Delta D}{\Delta \beta_1} \right) \frac{d\beta_1}{dr_1} \right] \Delta r_1 \quad (\text{B88})$$

meas - D:r<sub>2</sub> (eqs. (B86) and (B87))

$$\Delta D = - \left[ \left( \frac{\Delta D}{\Delta V_2} \right) \frac{dV_2}{dr_2} + \left( \frac{\Delta D}{\Delta \beta_2} \right) \frac{d\beta_2}{dr_2} \right] \Delta r_2 \quad (\text{B89})$$

meas - D:U<sub>t</sub> (In fig. 2(c), substitute  $\beta'_1$  for  $\beta_2$ ,  $\beta_1$  for  $\beta'_2$ , and multiply result by  $(1 - D)$ . Then substitute  $\beta'_2$  for  $\beta_2$ ,  $\beta_2$  for  $\beta'_2$ , multiply by  $V'_2/V'_1$ , and subtract from previous result.)

$$\Delta D = \left[ (1 - D) \sin \beta'_1 \cos \beta'_1 (\tan \beta'_1 + \tan \beta_1) - \frac{V'_2}{V'_1} \sin \beta'_2 \cos \beta'_2 (\tan \beta'_2 + \tan \beta_2) \right] \frac{\Delta U_t}{U_t} \quad (\text{B90})$$

meas -  $k:V_1$  (See fig. 2(a). Substitute  $\beta'_1$  for  $\beta_2$ ,  $\beta_1$  for  $\beta'_2$ , multiply result by  $-2k$ , and add 2 times result of fig. 3(b).)

$$\Delta k = 2 \left[ k \cos^2 \beta'_1 (\tan \beta'_1 \tan \beta_1 - 1) - \cos^2 \beta'_1 \sec^2 \beta_1 \right] \frac{\Delta V_1}{V_1} \quad (\text{B91})$$

$$\Delta k = -2(1 + k) \cos^2 \beta'_1 \frac{\Delta V_1}{V_1} \quad \text{for } \beta_1 = 0$$

meas -  $k:\beta_1$  (See fig. 8(b). Substitute  $\beta'_1$  for  $\beta'_2$  and  $\beta_1$  for  $\beta_2$ , and multiply result by  $k$ .)

$$\Delta k = k \frac{\pi}{90} \cos^2 \beta'_1 (\tan \beta'_1 + \tan \beta_1) \Delta \beta_1 \quad (\text{B92})$$

$$\Delta k = k \frac{\pi}{180} \sin 2\beta'_1 \Delta \beta_1 \quad \text{for } \beta_1 = 0$$

meas -  $k:r_1$  (See fig. 2(c). Substitute  $\beta'_1$  for  $\beta_2$  and  $\beta_1$  for  $\beta'_2$ , multiply by  $-2k$ , and subtract  $(1/r_1)(dk/dr_1)$ .)

$$\Delta k = - \left[ 2k \sin \beta'_1 \cos \beta'_1 (\tan \beta'_1 + \tan \beta) + r_1 \frac{dk}{dr_1} \right] \frac{\Delta r_1}{r_1} \quad (\text{B93})$$

meas -  $k:H_{sv}$

$$\Delta k = \frac{2g}{V_1'^2} \Delta H_{sv} \quad (\text{B94})$$

## APPENDIX C

### APPLICATION OF THE MEASUREMENT ERROR ANALYSIS TO SPECIFIC TEST DATA

Two data points were selected for use in this example: the design point of the highly loaded axial rotor of references 3 and 4 and a typical operating point for the 84° helical inducer of reference 5. The rotor design point had an overall  $\phi$  of 0.451 and an overall  $\psi$  of 0.391, and the inducer operating point had an overall  $\phi$  of 0.0656 and an overall  $\psi$  of 0.117. For both of these points, the flow was noncavitating. The 84° inducer has near the highest blade angle used in current pump designs, whereas the rotor of references 3 and 4 has relatively low blade angles because of the high flow coefficient, and also has high loading.

The values of measurement accuracy used in this example are estimates which include the effects of more sources of error than just the instrumentation accuracies as given in references 4 and 5. The possible sources of error (pressure and flow fluctuations, etc.) are discussed in the CONCLUDING REMARKS section of this report. The results should give an idea of what accuracy to expect in current pump test data. The measurement errors assumed in this study are listed in table III.

TABLE III. - MEASURED ERROR ESTIMATES

[Angle,  $\pm 1^\circ$ ; radius, 1 percent of passage height.]

Measured variable	Highly loaded rotor (a)		84° Inducer (a)	
	$\pm ft$	$\pm m$	$\pm ft$	$\pm m$
Head rise	4 (180)	1.2 (55)	7 (210)	2 (64)
Inlet pressure	3 <sup>b</sup> (240)	.9 <sup>b</sup> (73)	.5 <sup>b</sup> (70)	.15 <sup>b</sup> (21)
Inlet velocity head	1.5 (49)	.5 (15)	.5 (4.2)	.15 (1.3)
Outlet velocity head	3 (120)	.9 (37)	2 (58)	.6 (18)

<sup>a</sup> Parenthetical values are maximum readings at the test points.

<sup>b</sup> Absolute.

Using these estimates of the measurement errors, the amounts of error in the performance parameters due to the various measurement errors were calculated. The results are shown in figures 10 to 15 for the performance parameters  $\psi_i$ ,  $\psi$ ,  $\bar{\omega}$ ,  $\delta$ , and  $\varphi_2$ , and the measurements of  $\beta_1$ ,  $V_2$ ,  $\beta_2$ , and  $\Delta H$ . These figures show the performance data with solid lines outlining the limits of probable error as calculated from the error equations.

To illustrate the computations, consider the errors in  $\delta$  (or  $\beta'_2$ ) due to errors in  $V_2$  for the highly loaded rotor. The sensitivity of  $\delta$  to errors in  $V_2$  is given in equation  $\text{meas} - \beta'_2:V_2$  and figure 3(a). This figure shows that for  $r_2 = 4.26$  inches (10.8 cm) at design flow, where  $\beta_2 = 41.7^\circ$  and  $\beta'_2 = 49.0^\circ$ , a 1 percent error in  $V_2$  will give a  $-0.51^\circ$  error in  $\delta$ . From the error of  $\pm 3$  feet (0.9 m) in 84 feet (26 m) of outlet velocity head (corresponding to a  $V_2$  of 73.5 ft/sec (22.4 m/sec)), the error in  $V_2$  is 1.8 percent. This error in  $V_2$  results in a  $\pm 0.9^\circ$  error in  $\delta$ . The corresponding limits of probable error are shown as solid lines in figure 14(a), which, for the radius  $r_2 = 4.26$  inches (10.8 cm), pass through  $\delta = 16.75^\circ + 0.9^\circ$  and  $\delta = 16.75^\circ - 0.9^\circ$ .

Figures 10 to 14 show the uncertainty intervals in the performance parameters due to individual measurement errors. The differences in the relative magnitude of errors in comparing the rotor performance to the inducer performance may be due either to differences in the accuracy of the measurements or to differences in the sensitivity to measurement errors. In figure 13(a), the larger uncertainty intervals in  $\varphi_2$  for the inducer (when compared on the basis of percentage of the nominal  $\varphi_2$  value) are a result of the poorer percentage accuracy assumed for the inducer  $V_2$  measurement. The other discernable differences in figures 10 to 14 can be explained by the effects of a change in stagger angle on the sensitivity to errors; these effects are listed in table II. For example, figures 10(a) and (c) show that the errors in  $\psi_i$  due to measurement errors in  $\beta_1$  and  $\beta_2$  are smaller for the inducer; this agrees with the predicted trend of less sensitivity at high stagger angles. The same trend for  $\bar{\omega}$  appears in figures 12(a) and (c). Further examples are the greater errors in  $\varphi_2$  and  $\delta$  due to errors in  $\beta_2$  for the inducer, and the reduced errors in  $\delta$  due to errors in  $V_2$ .

Another item of interest is the relative importance of the different measurement errors in contributing to the total errors of the various performance parameters. For the highly loaded rotor,  $\beta_1$ ,  $V_2$ , and  $\beta_2$  contribute about equally to errors in  $\psi_i$  (figs. 10(a) to (c)). But for the inducer, the influence of  $\beta_1$  and  $\beta_2$  errors is diminished, leaving the  $V_2$  measurement as the main source of error in  $\psi_i$ . The situation is similar for the performance parameters  $\bar{\omega}$  (figs. 12(a) to (d)) and  $\eta$  (not shown), where the  $\beta_1$ ,  $\beta_2$ ,  $V_2$ , and  $\Delta H$  measurements contribute about equal errors for the conventional rotor performance, but only the  $V_2$  and  $\Delta H$  measurements are important sources of error for the inducer performance. In fact, for the inducer,  $V_2$  was the main source of error for most of the performance parameters. To get better data, improving this particular measurement would be of prime importance. For the highly



loaded rotor, no one measurement could be singled out as being the greatest source of error.

Since the errors in rotative speed are negligible, the errors in  $\psi$  (fig. 11) are caused almost entirely by errors in the measurement of head rise. Consequently, there is no change of sensitivity with blade angle. The percentage errors in  $\psi$  are about the same for the rotor and the inducer, although the different scales of the graphs make them appear different.

For the test configurations used, there was no energy addition upstream of the blade inlet, so the errors in  $\beta_1$  do not actually affect the  $\psi_i$  values and have a smaller effect on the  $\bar{\omega}$  values than shown in figure 12(a). However, under other conditions the relative size of the errors due to  $\beta_1$  might be important, so the curves are included for comparison purposes. For all the performance parameters, the effect of radial probe positioning errors were small, and are not shown in the figures. Also, for  $\beta_1$  nearly equal to zero, the effect of errors in  $V_1$  are negligible.

The errors in the performance parameters due to the combined effects of all measurement errors are shown in figure 15. Equation (3) is used to calculate the total amount of error, as it is assumed that all of the measurement errors are random in nature. Thus the solid lines in the figures show the uncertainty intervals in the performance parameters. As errors in  $\beta_1$  did not actually affect the values of  $\psi_i$  and had only a slight effect on the values of  $\bar{\omega}$ , those particular errors were not included in the calculations. It is interesting to note that the errors in  $\psi$  and  $\psi_i$  are about the same. Although the magnitude of the errors in deviation angle are smaller for the inducer, they are probably just as critical because of the greater sensitivity to errors in deviation angle at high blade angles, as noted in the design error equations. No other significant differences were found between the magnitude of errors in the inducer and in the axial rotor.

An error analysis need not be restricted to the parameters considered herein. For the data of references 3 to 5, both the Venturi flow rate and the mass averaged parameters are amenable to error analysis techniques. The accuracy of the flow rate can be determined from estimates of the accuracy in the measurement of pressure across the Venturi. The errors in the mass averaged parameters can be determined using equation (3) to get the combined effect of individual errors at several radial positions. Both are relatively simple applications of error analysis techniques.

## REFERENCES

1. Jackson, Robert J.; and Yohner, Peggy L.: Effects of Design and Measurement Errors on Compressor Performance. Aerodynamic Design of Axial-Flow Compressors. Irving A. Johnsen and Robert O. Bullock, eds. NASA SP-36, 1965, pp. 413-468.
2. Kline, S. J.; and McClintock, F. A.: Describing Uncertainties in Single-Sample Experiments. Mech. Eng., vol. 75, no. 1, Jan. 1953, pp. 3-8.
3. Miller, Max J.; and Crouse, James E.: Design and Overall Performance of an Axial-Flow Pump Rotor with a Blade-Tip Diffusion Factor of 0.66. NASA TN D-3024, 1965.
4. Miller, Max J.; and Sandercock, Donald M.: Blade Element Performance of Axial-Flow Pump Rotor with Blade Tip Diffusion Factor of 0.66. NASA TN D-3602, 1966.
5. Anderson, Douglas A.; Soltis, Richard F.; and Sandercock, Donald M.: Performance of  $84^{\circ}$  Flat-Plate Helical Inducer and Comparison with Performance of Similar  $78^{\circ}$  and  $80.6^{\circ}$  Inducers. NASA TN D-2553, 1964.

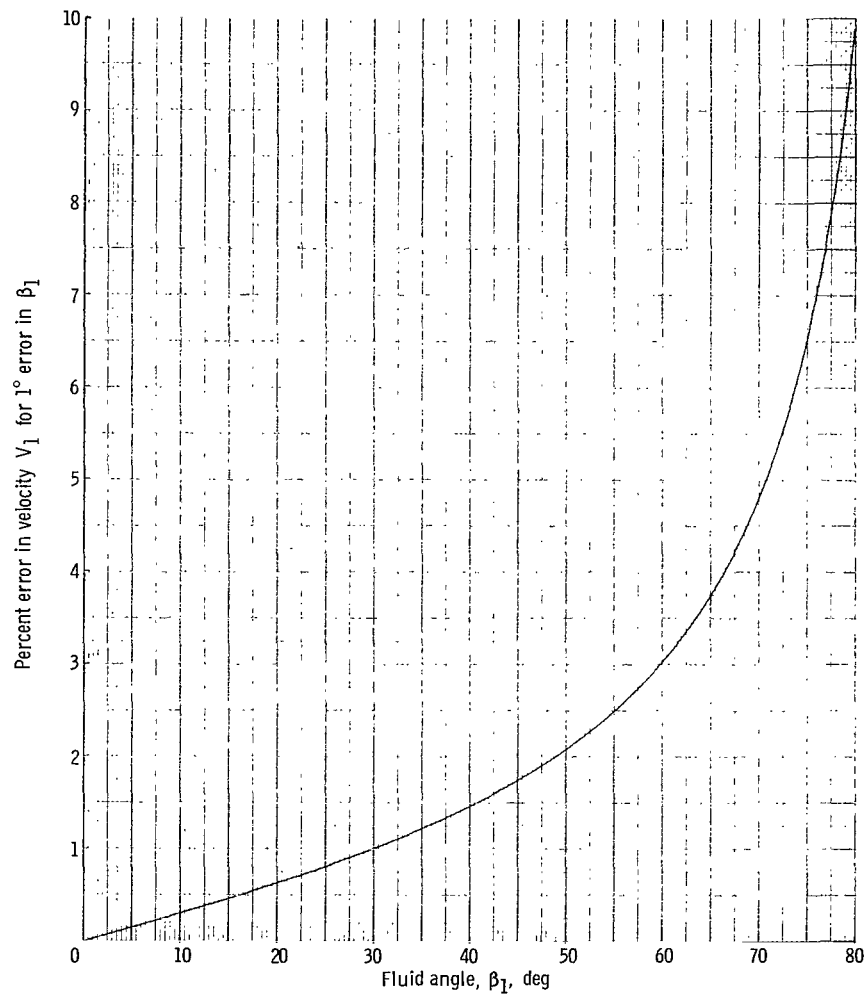


Figure 1. - Effect of design error in inlet flow angle on inlet velocity (eq. (B14)).

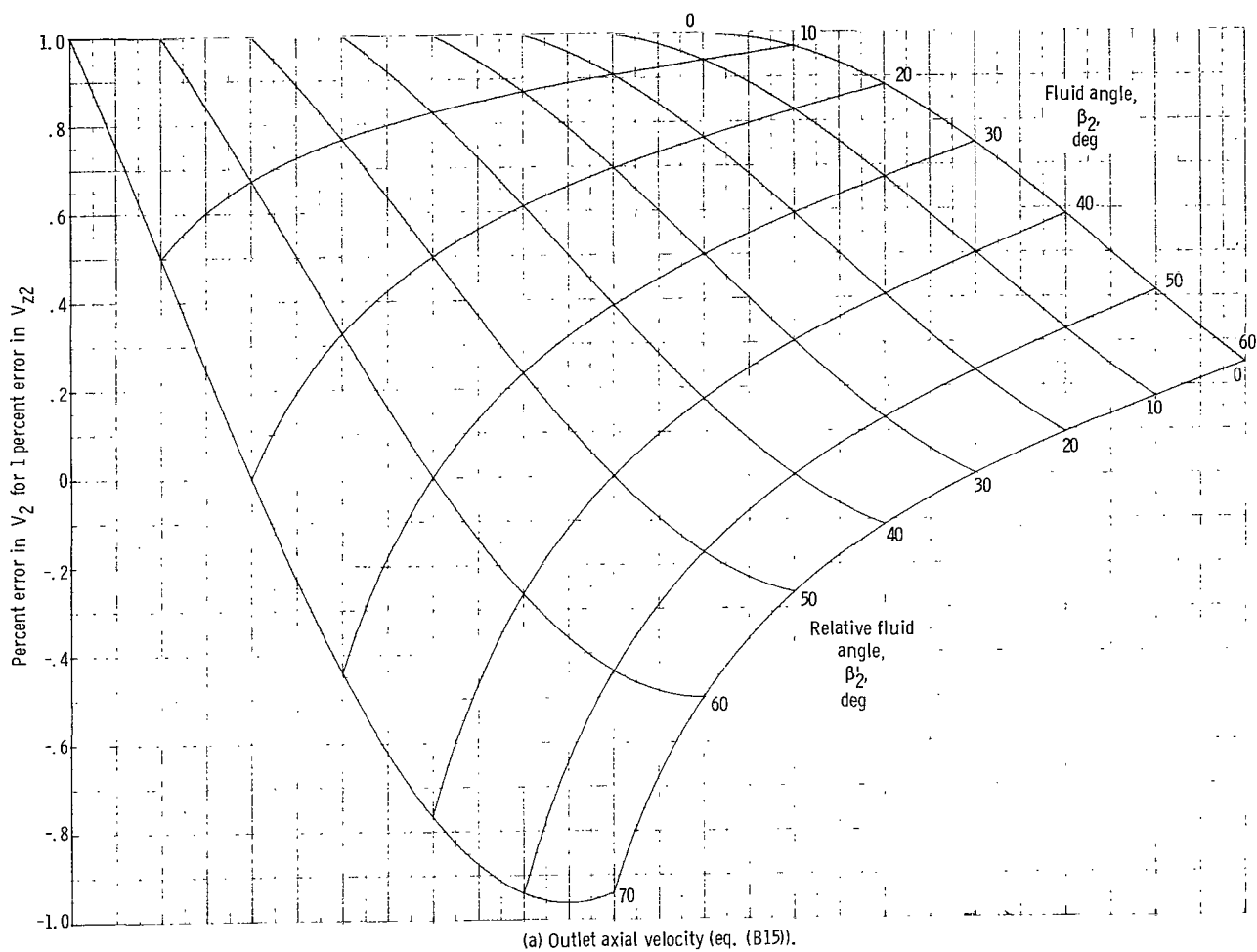
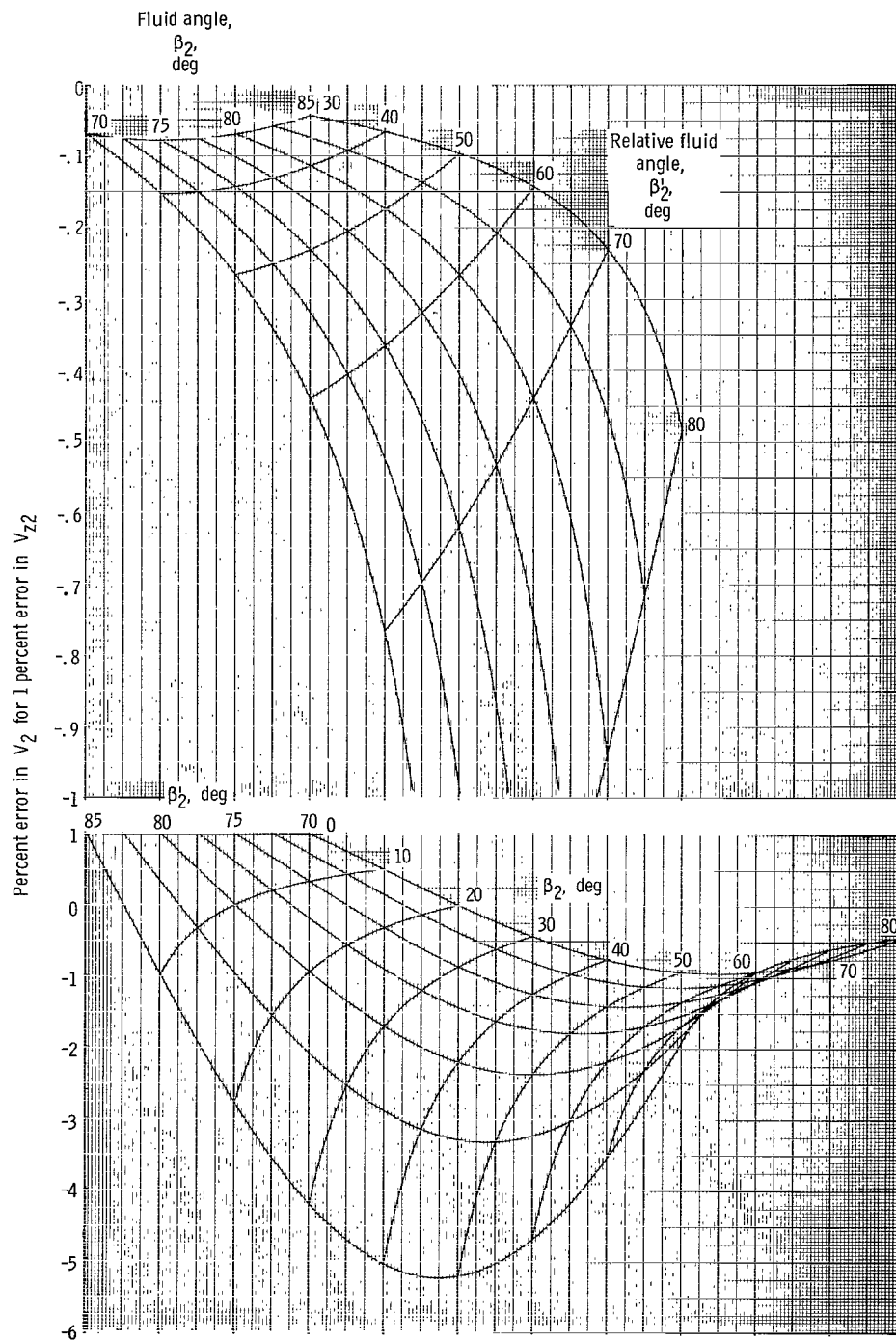
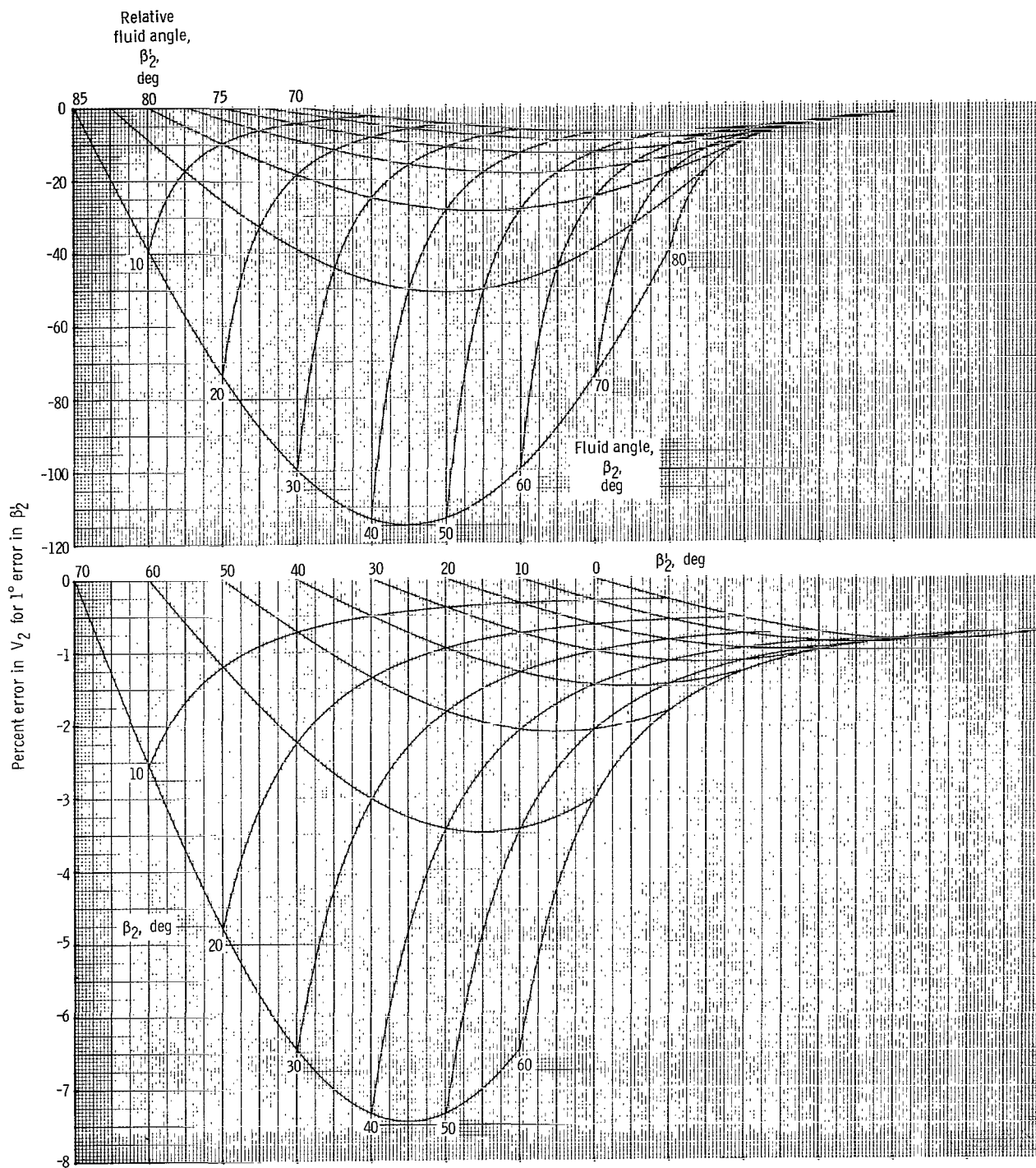


Figure 2. - Effect of design errors on outlet velocity.



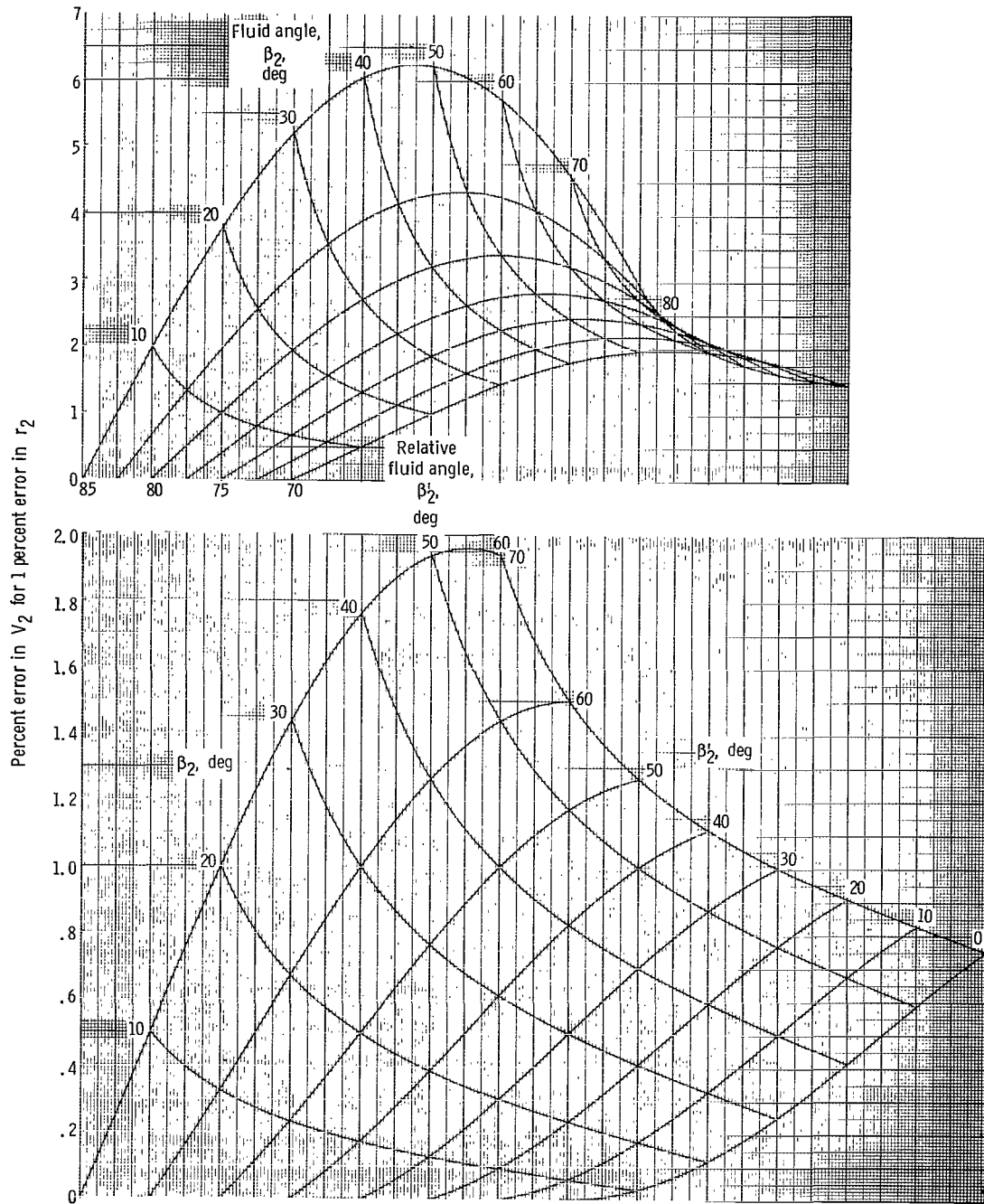
(a) Concluded.

Figure 2. - Continued.



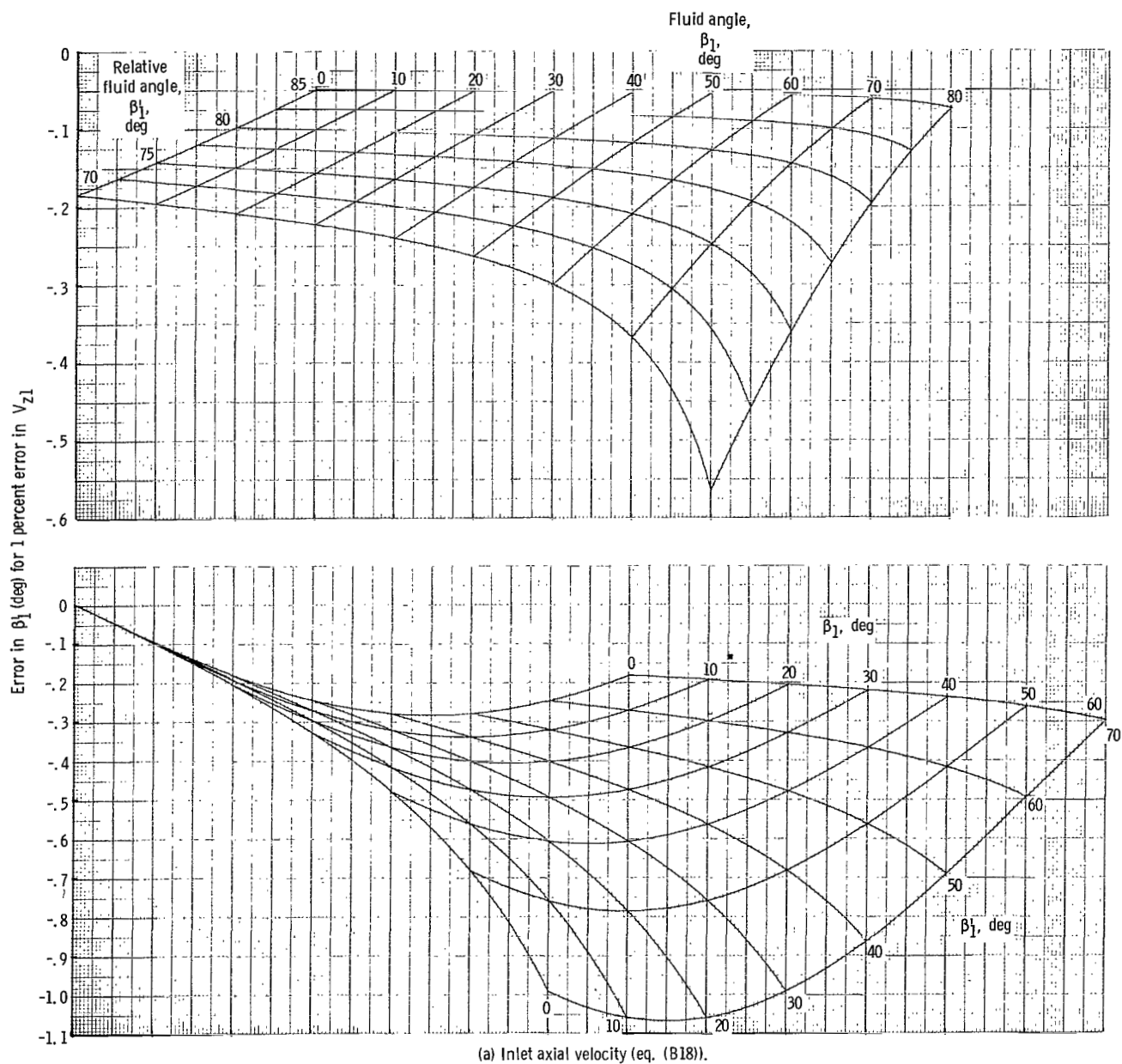
(b) Outlet relative flow angle (eq. (B16)).

Figure 2. - Continued.



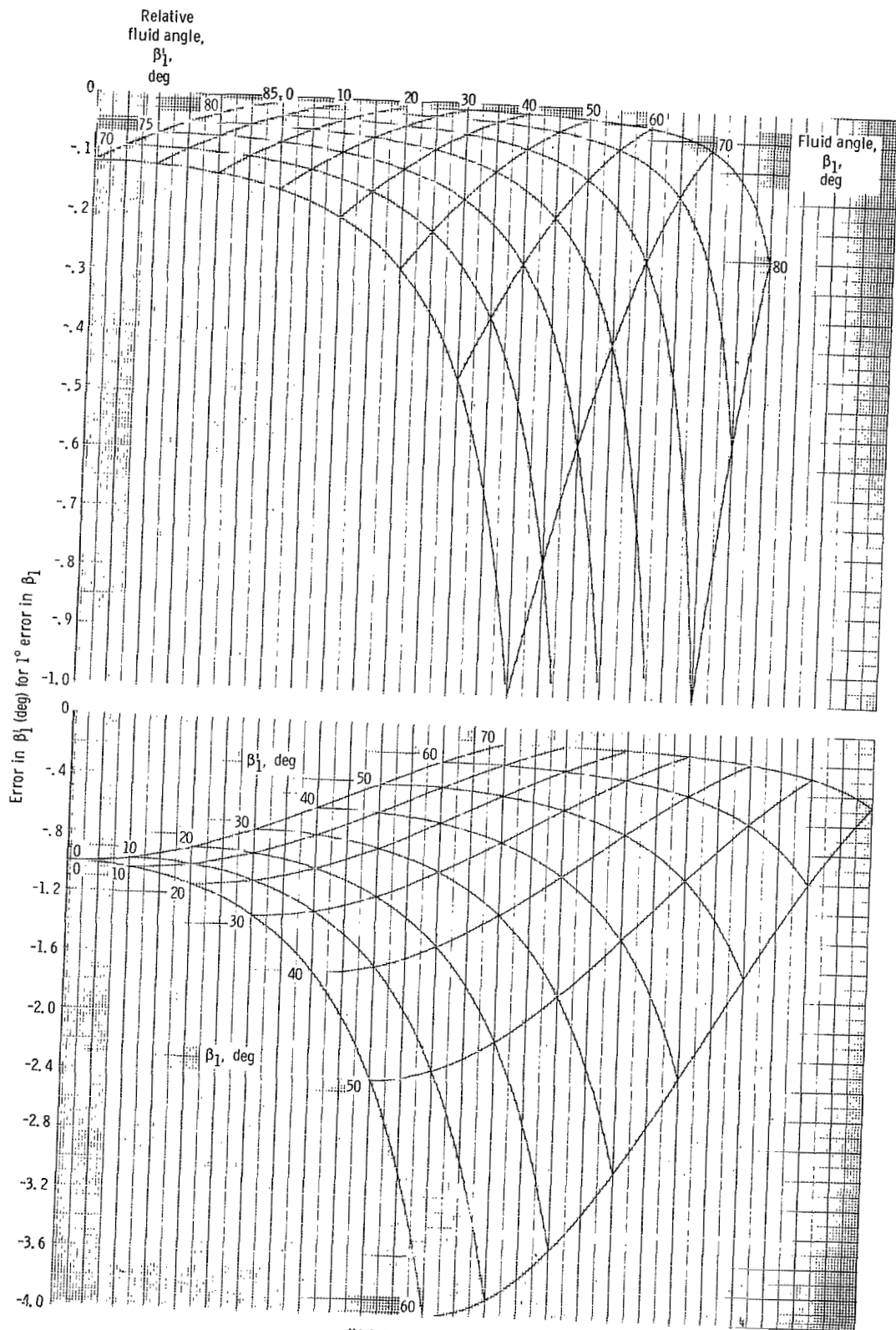
(c) Outlet radius (eq. (B17)).

Figure 2. - Concluded.



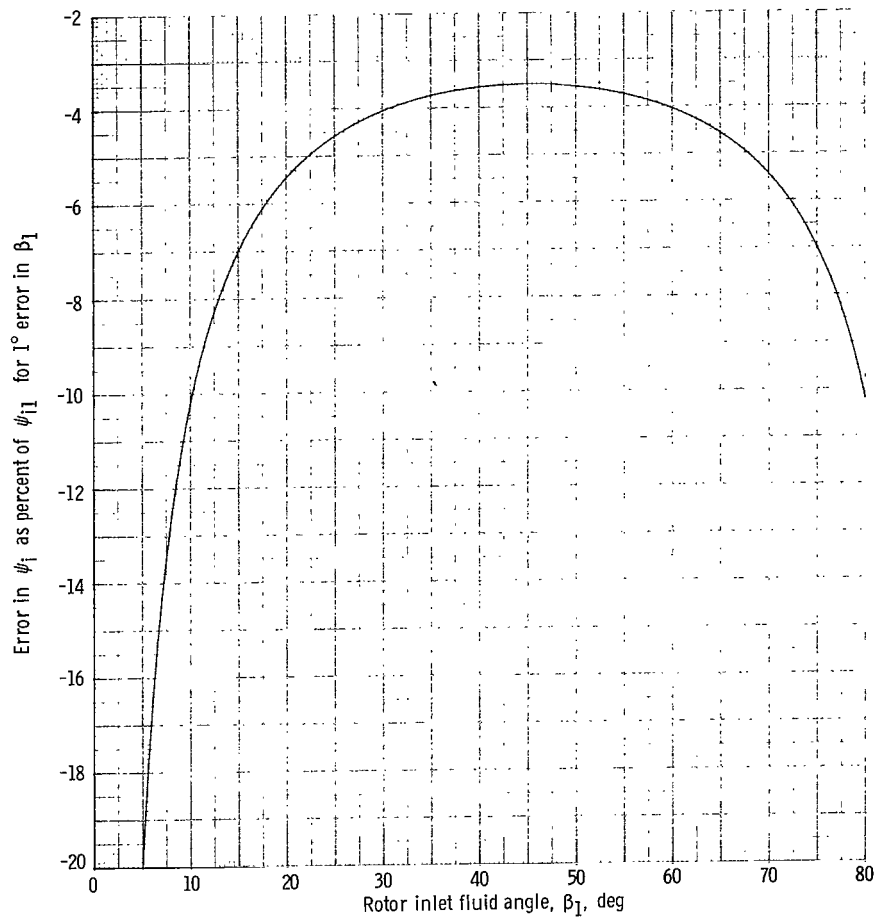
(a) Inlet axial velocity (eq. (B18)).  
Figure 3. - Effect of design errors on inlet relative flow angle.





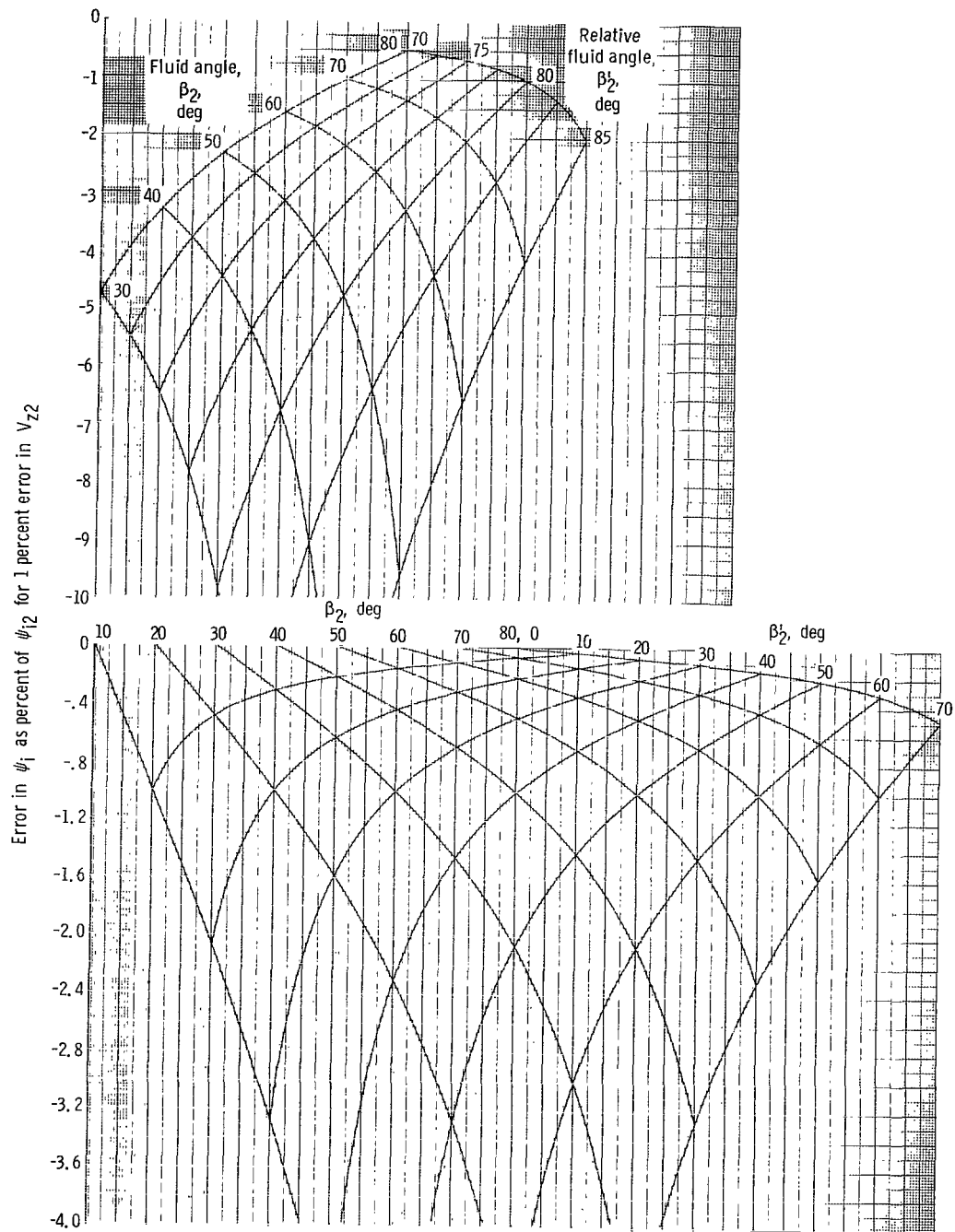
(b) Inlet fluid angle (eq. (B19)).

Figure 3. - Concluded.



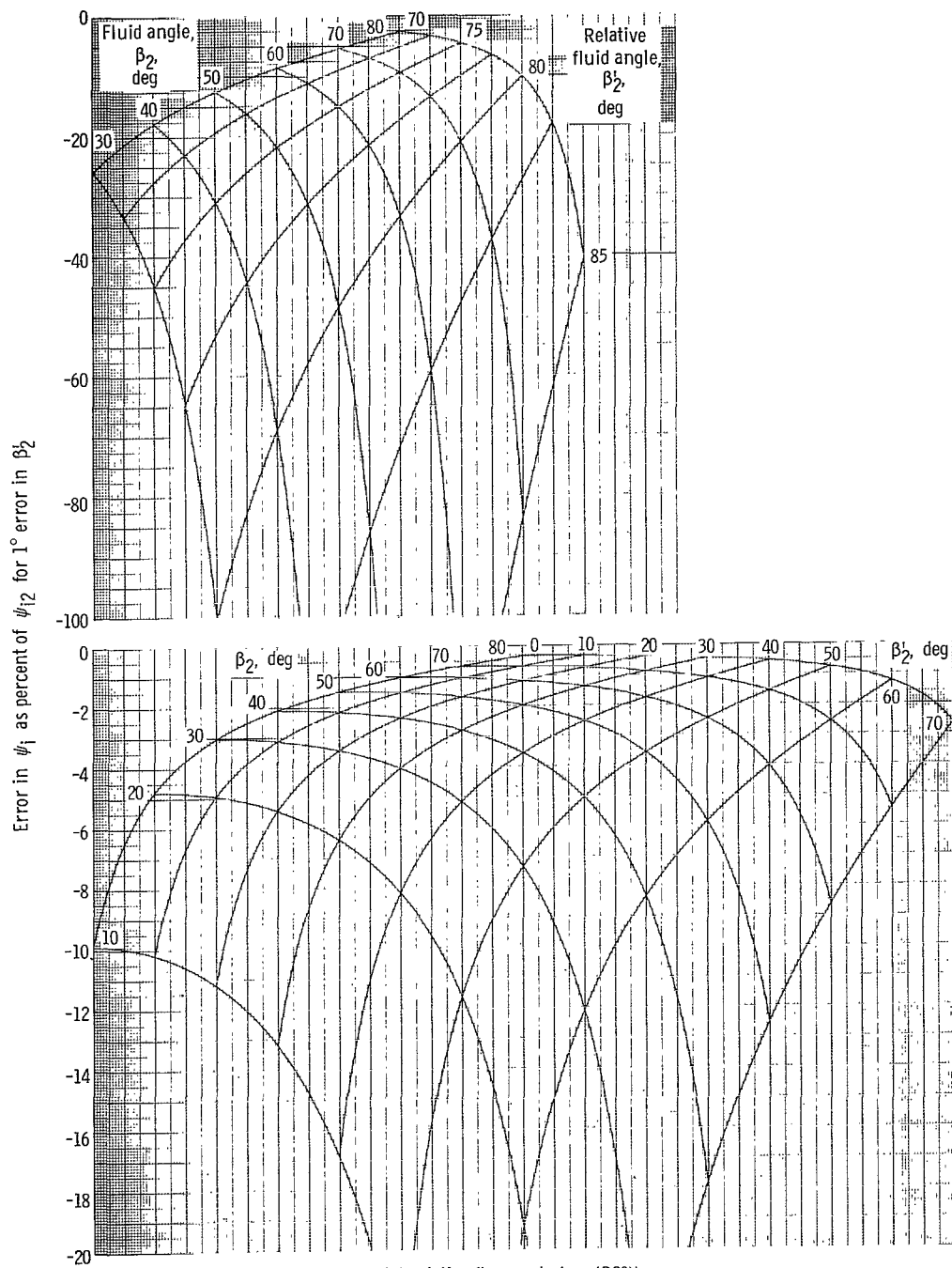
(a) Inlet flow angle (eq. (B25)).

Figure 4. - Effect of design errors on ideal head rise coefficient.



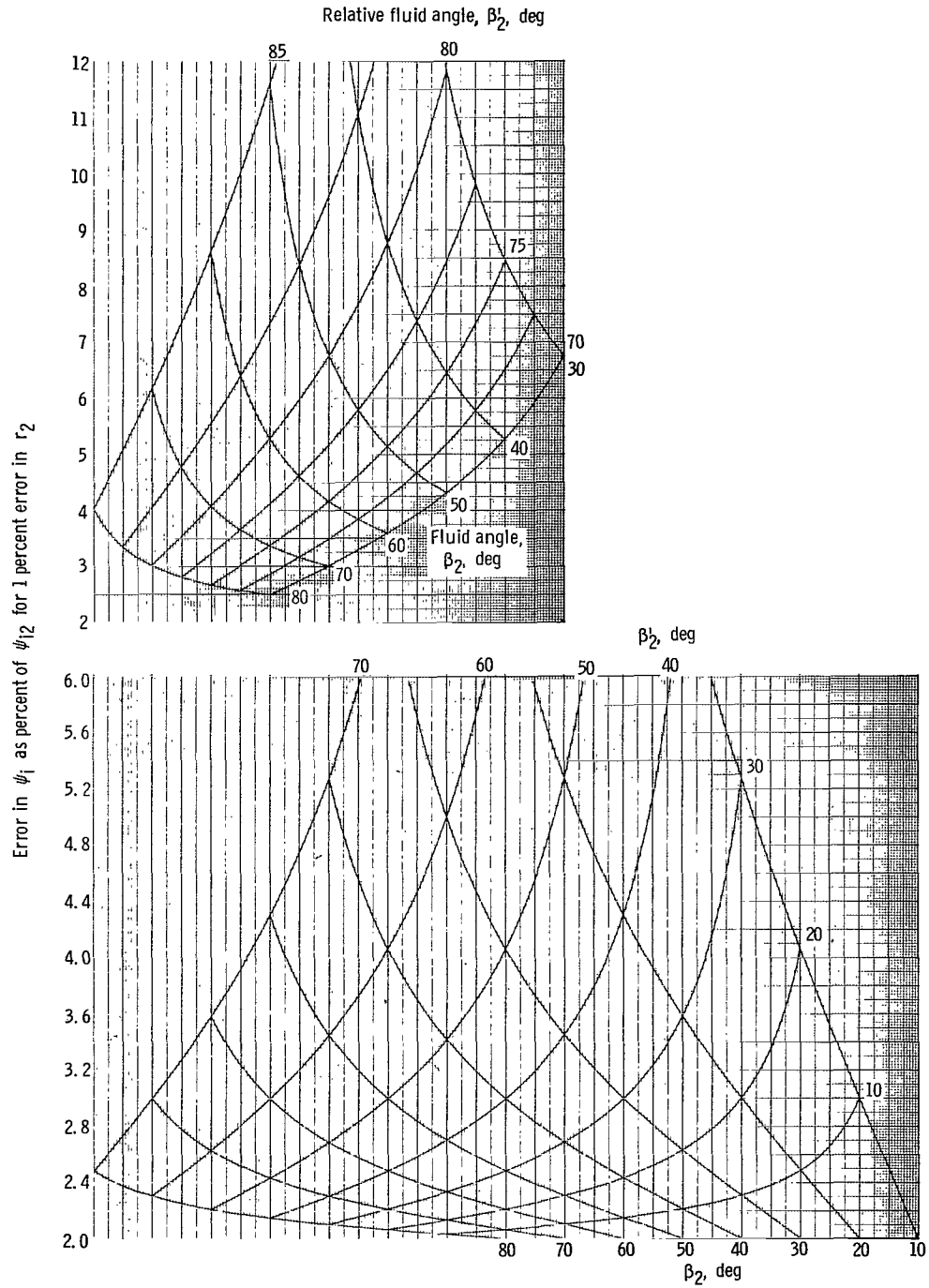
(b) Outlet axial velocity (eq. (B26)).

Figure 4. - Continued.



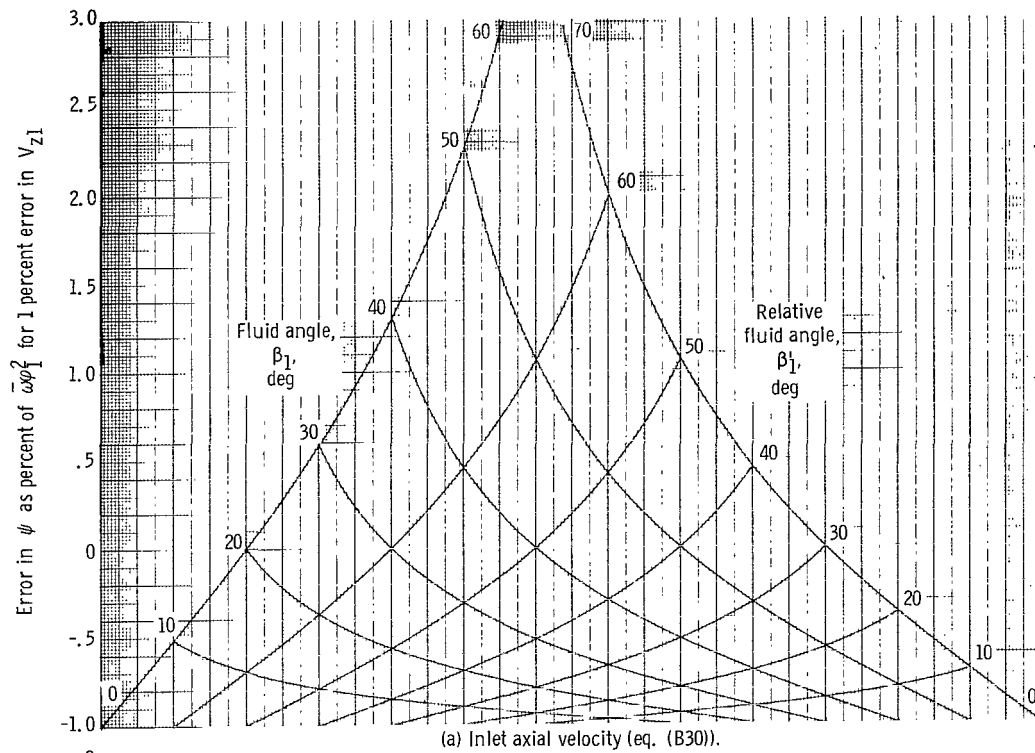
(c) Outlet relative flow angle (eq. (B28)).

Figure 4. - Continued.

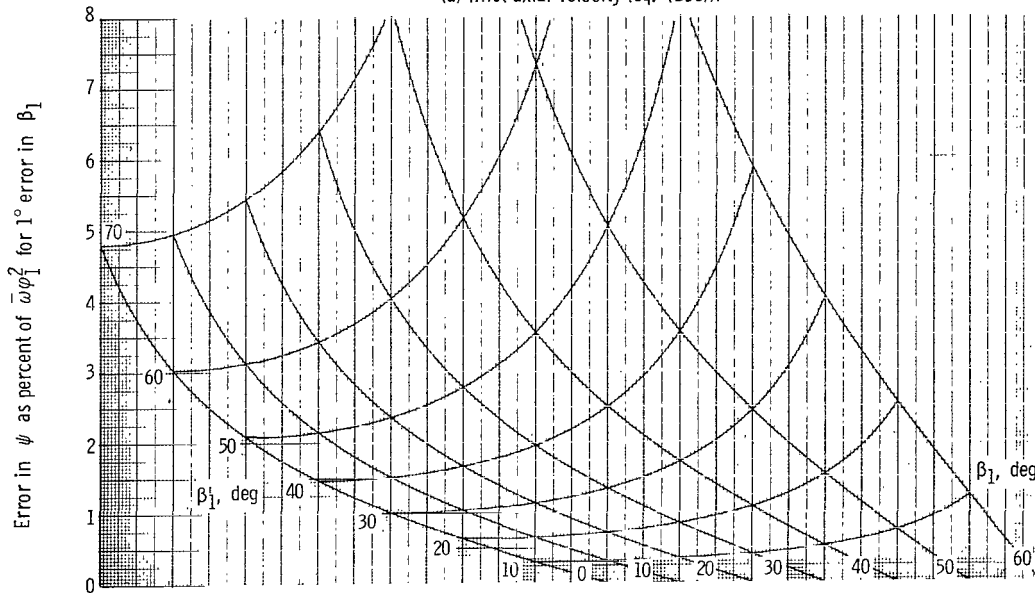


(d) Outlet radius (eq. (B29)).

Figure 4. - Concluded.

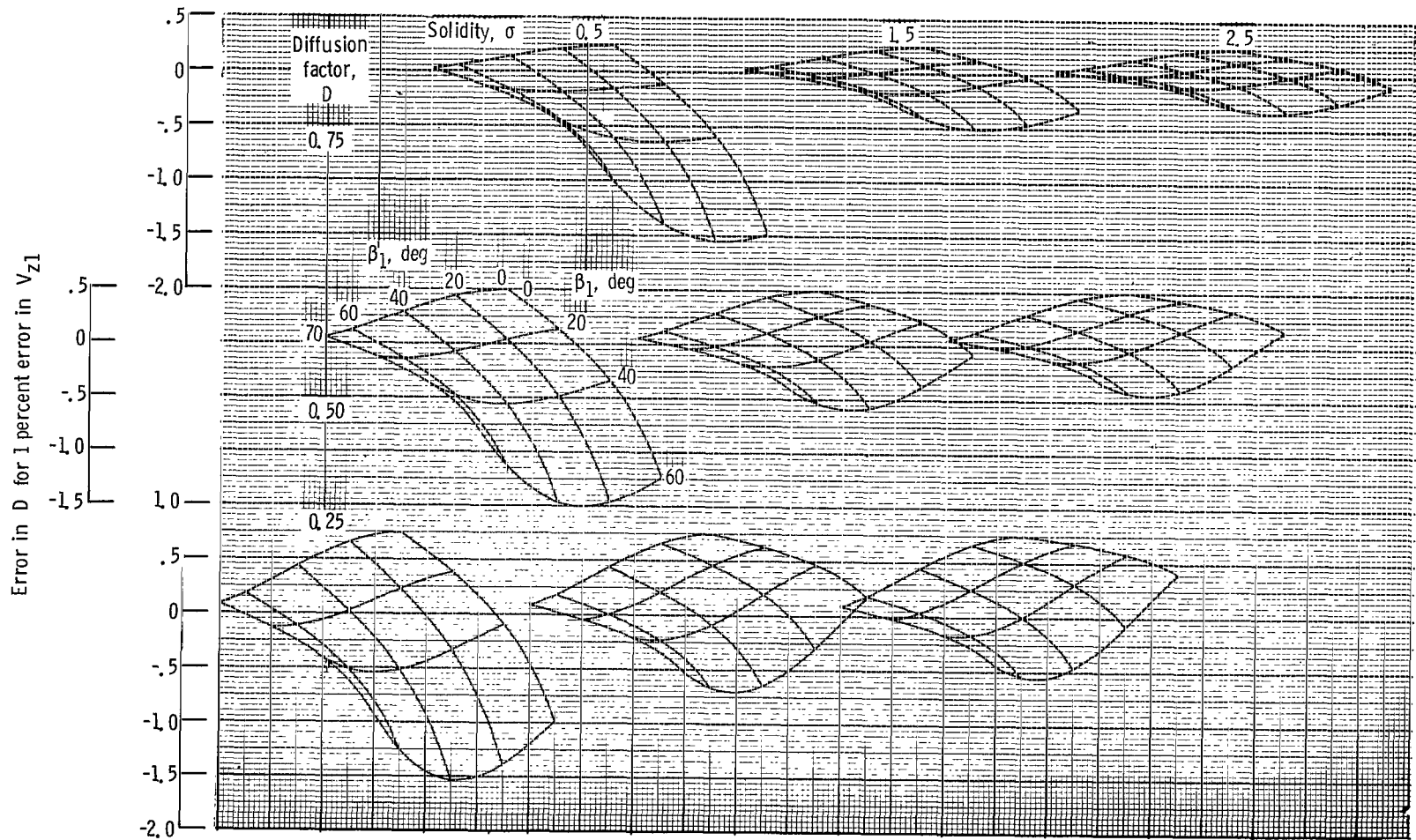


(a) Inlet axial velocity (eq. (B30)).



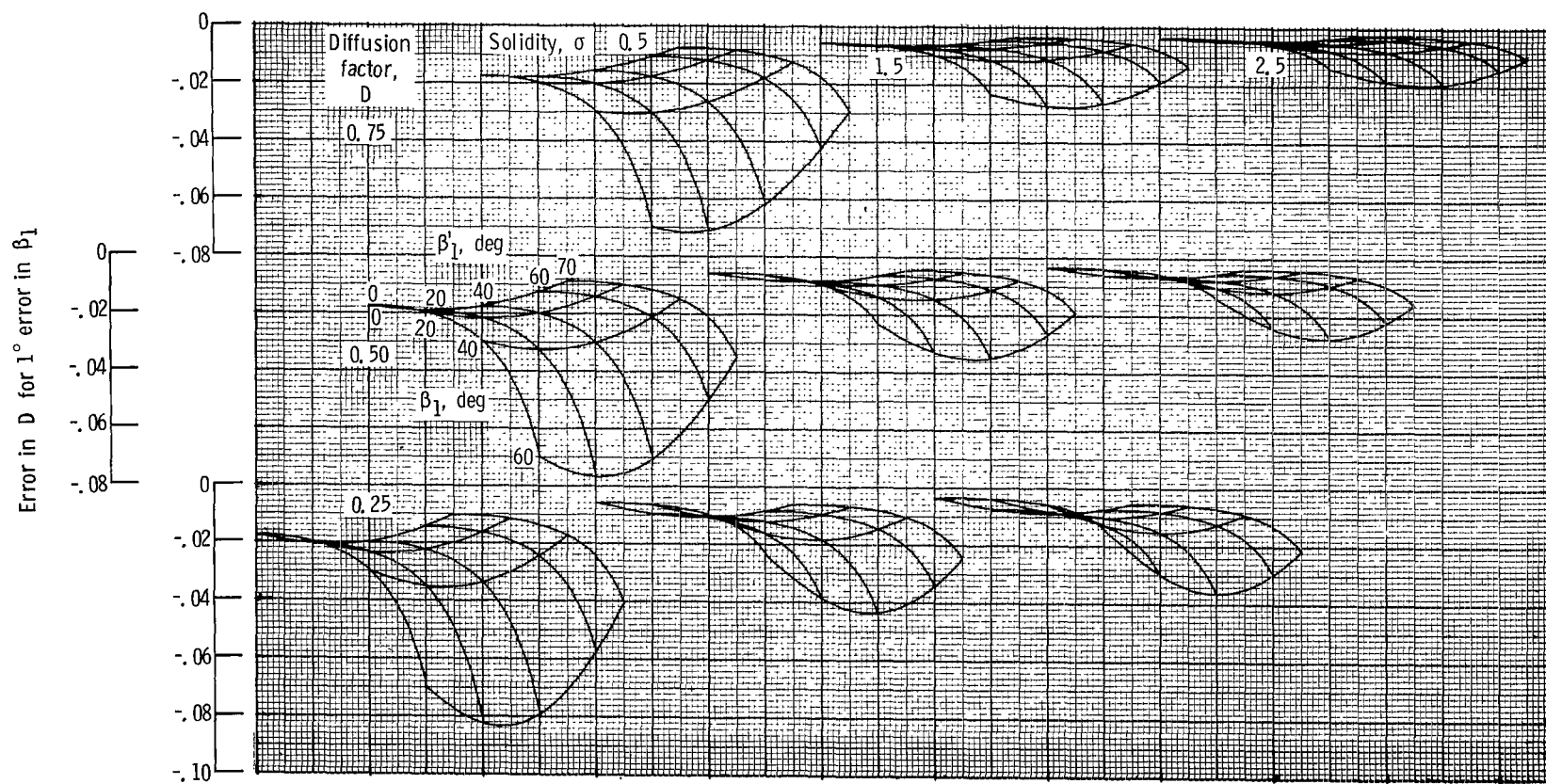
(b) Inlet fluid angle (eq. (B31)).

Figure 5. - Effect of design errors on head-rise coefficient.



(a) Inlet axial velocity (eq. (B38)).

Figure 6. - Effect of design errors on diffusion factor.



(b) Inlet flow angle (eq. (B39)).

Figure 6. - Continued.



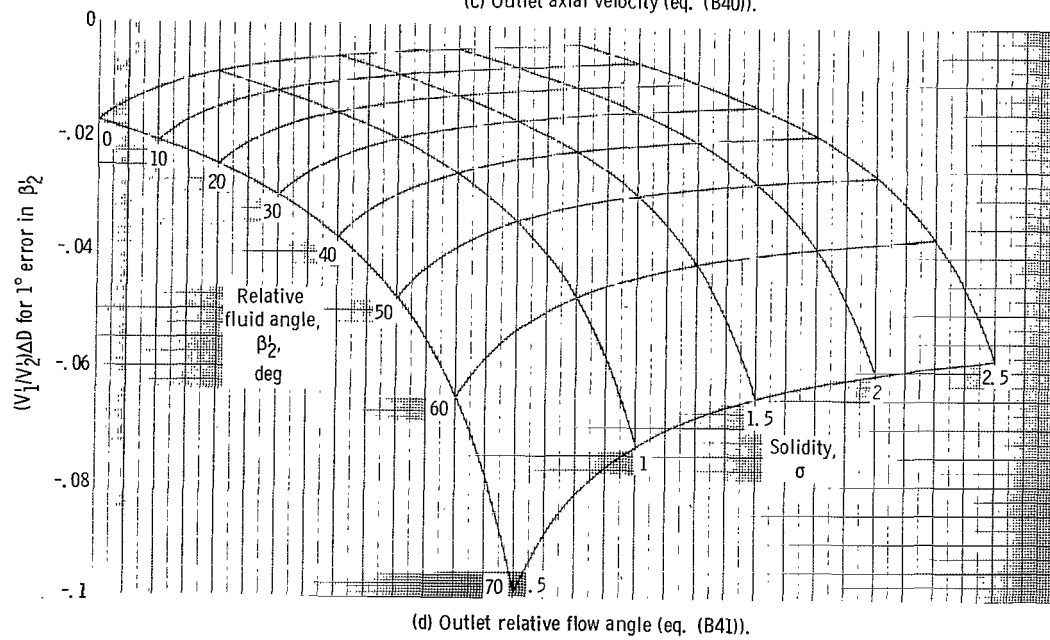
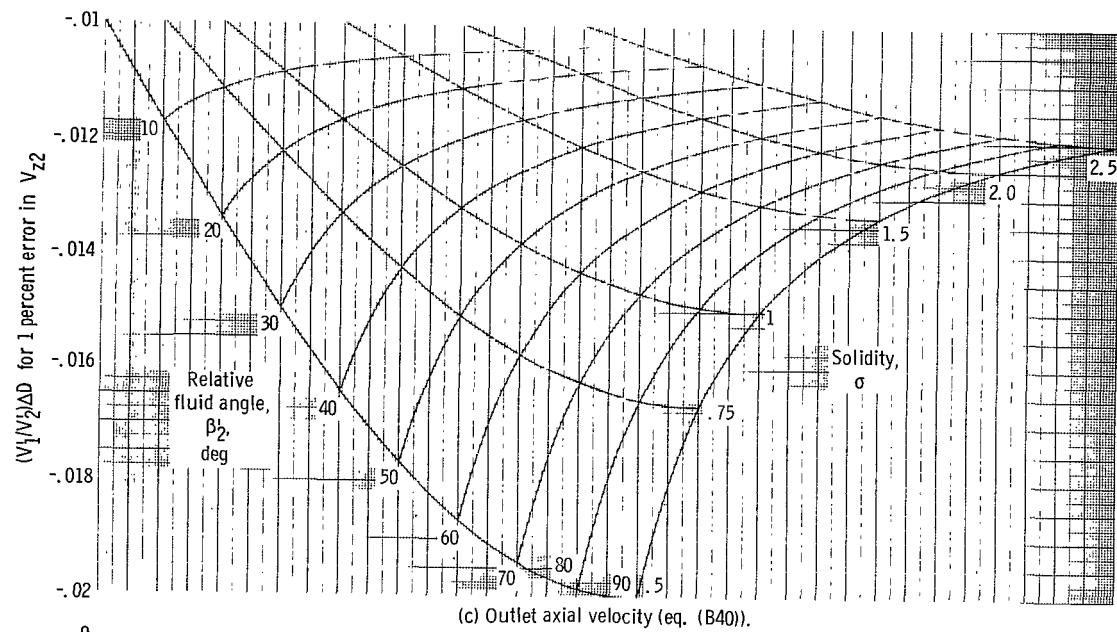
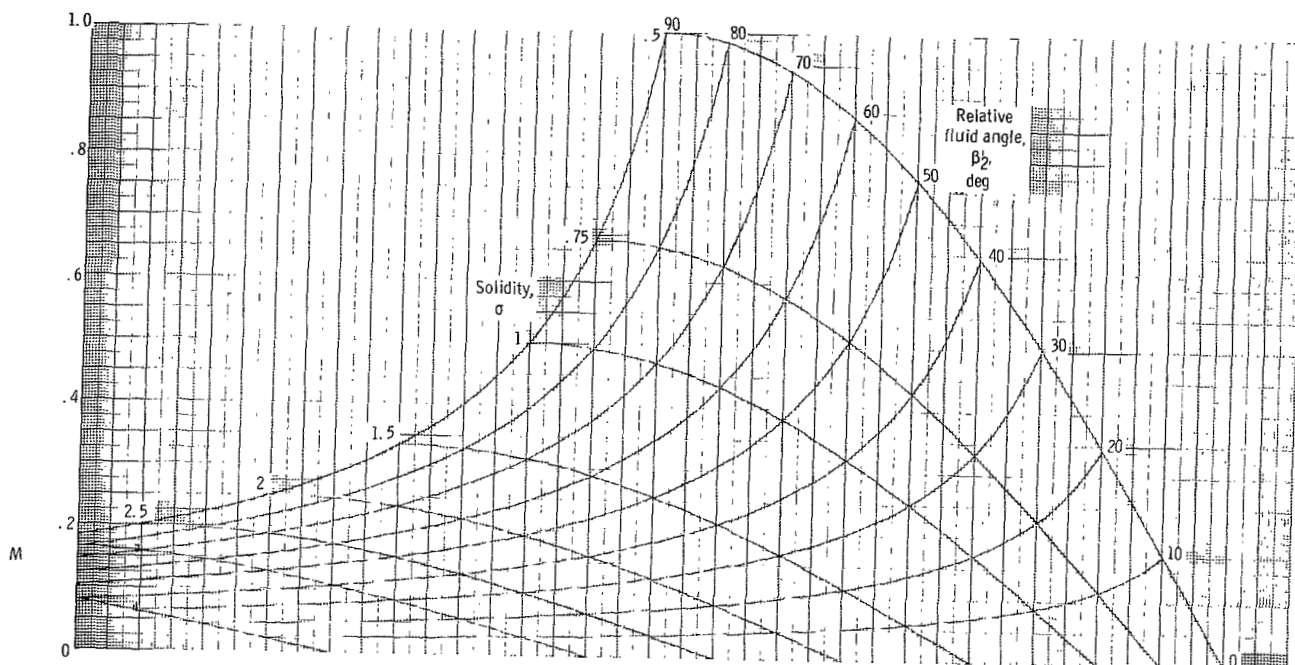
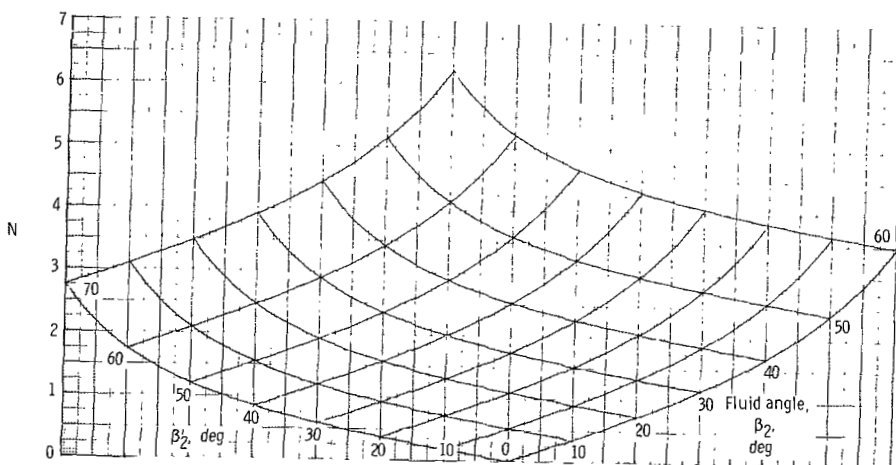


Figure 6. - Concluded.

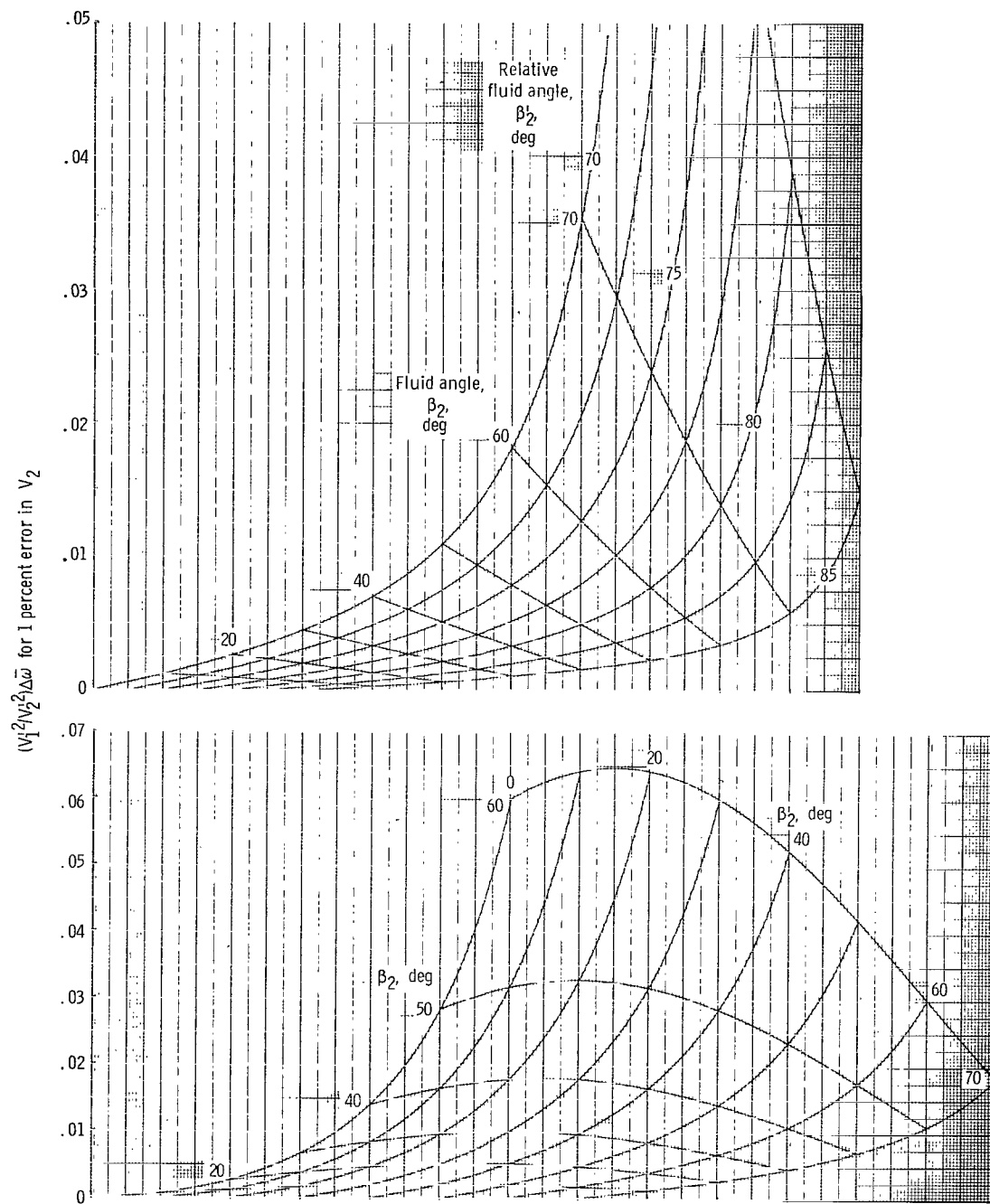


(a) Factor  $M$  (eqs. (B42) and (B43)).



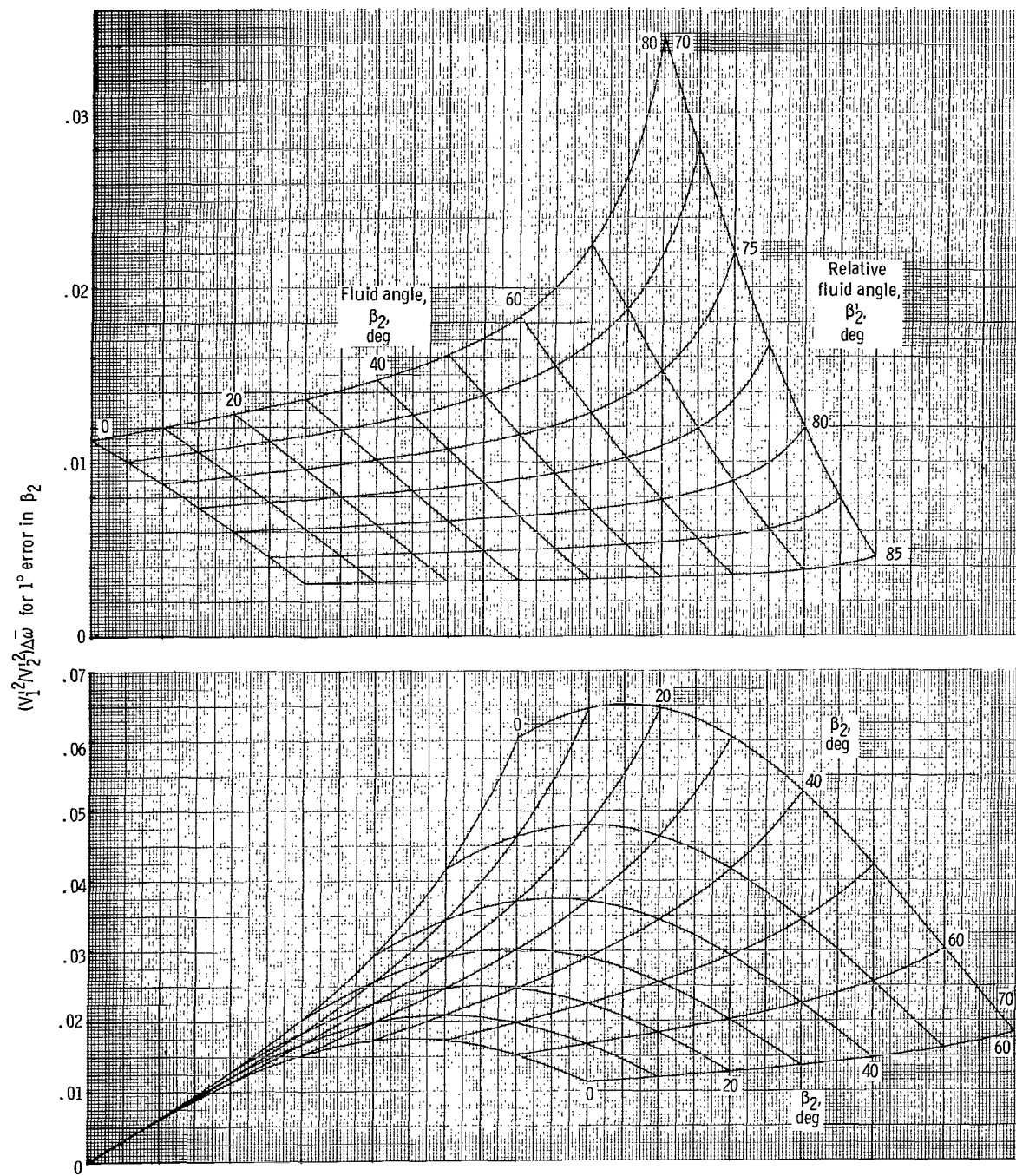
(b) Factor  $N$  (eqs. (B42) and (B44)).

Figure 7. - Factors  $M$  and  $N$  as functions of  $\beta_2$ ,  $\beta_2'$ , and  $\sigma$ .



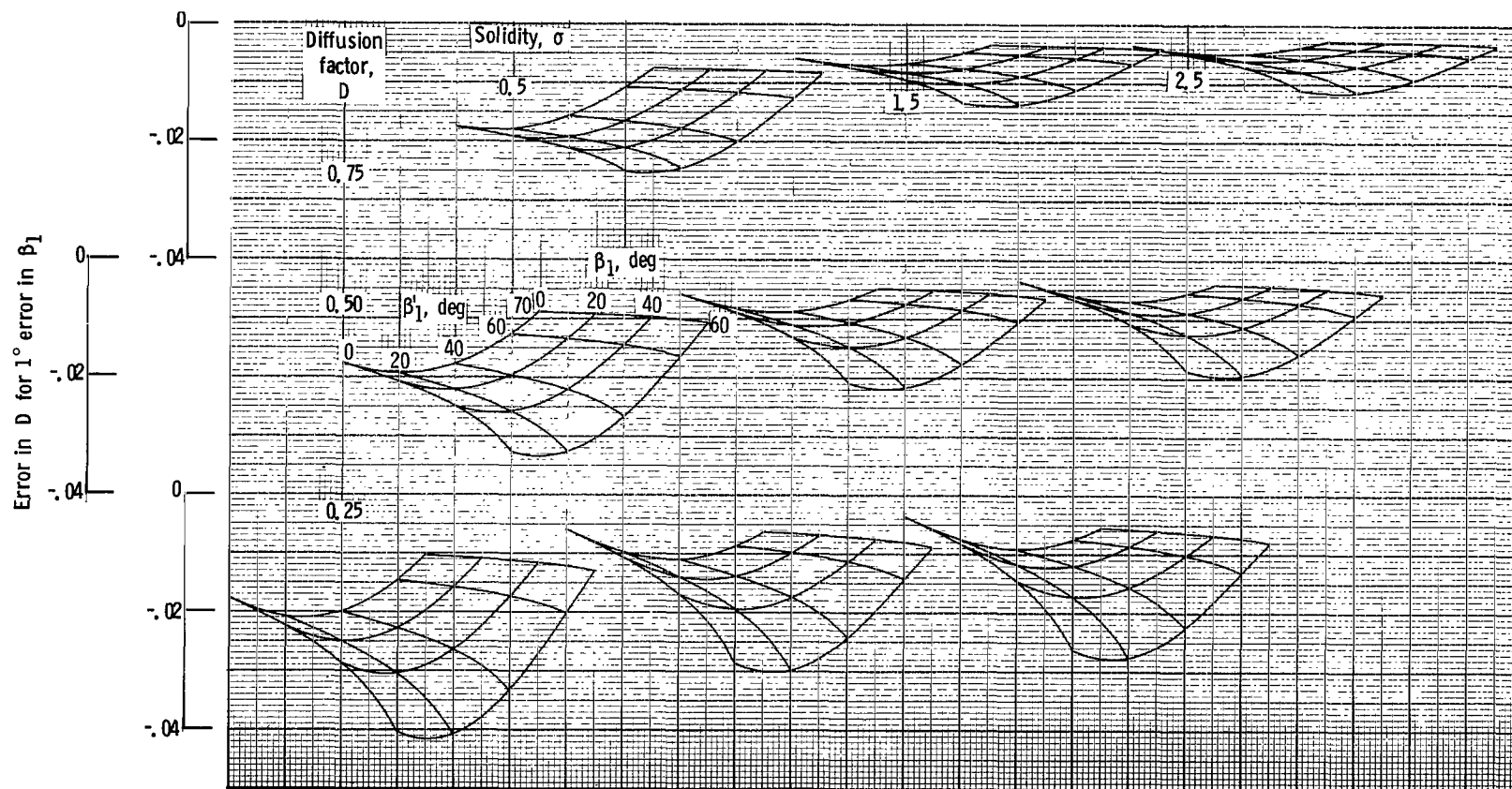
(a) Outlet velocity (eq. (B78)).

Figure 8. - Effect of measurement errors on loss coefficient.



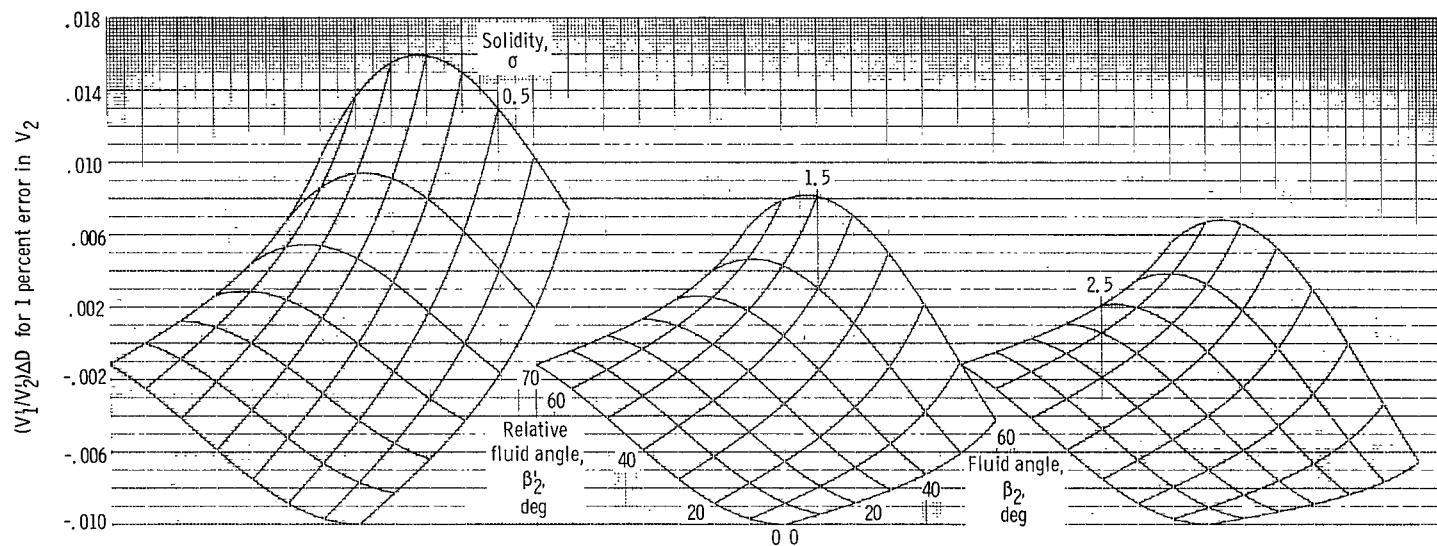
(b) Outlet fluid angle (eq. (B79)).

Figure 8. - Concluded.

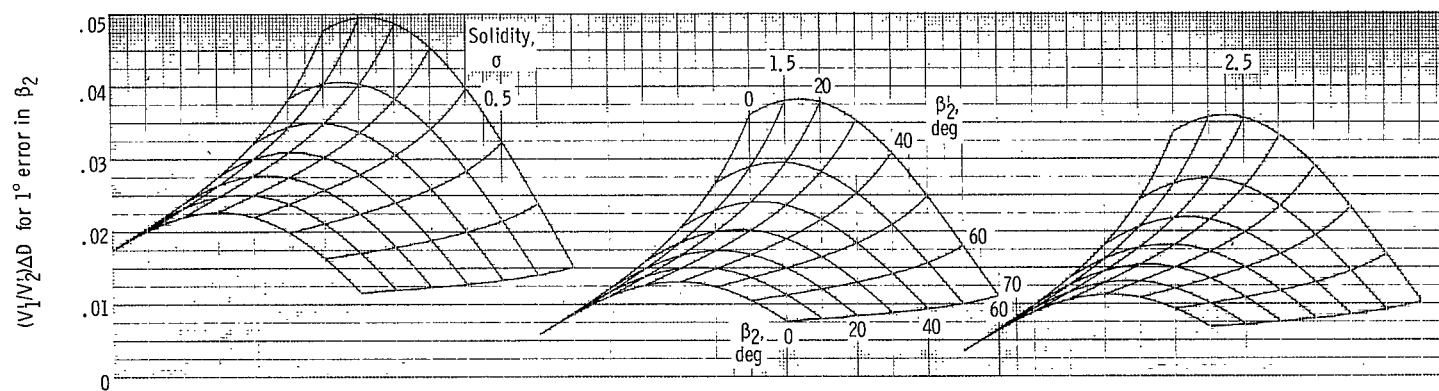


(a) Inlet fluid angle (eq. (B85)).

Figure 9. - Effect of measurement errors on diffusion factor.



(b) Outlet velocity (eq. (B86)).



(c) Outlet flow angle (eq. (B87)).

Figure 9. - Concluded.

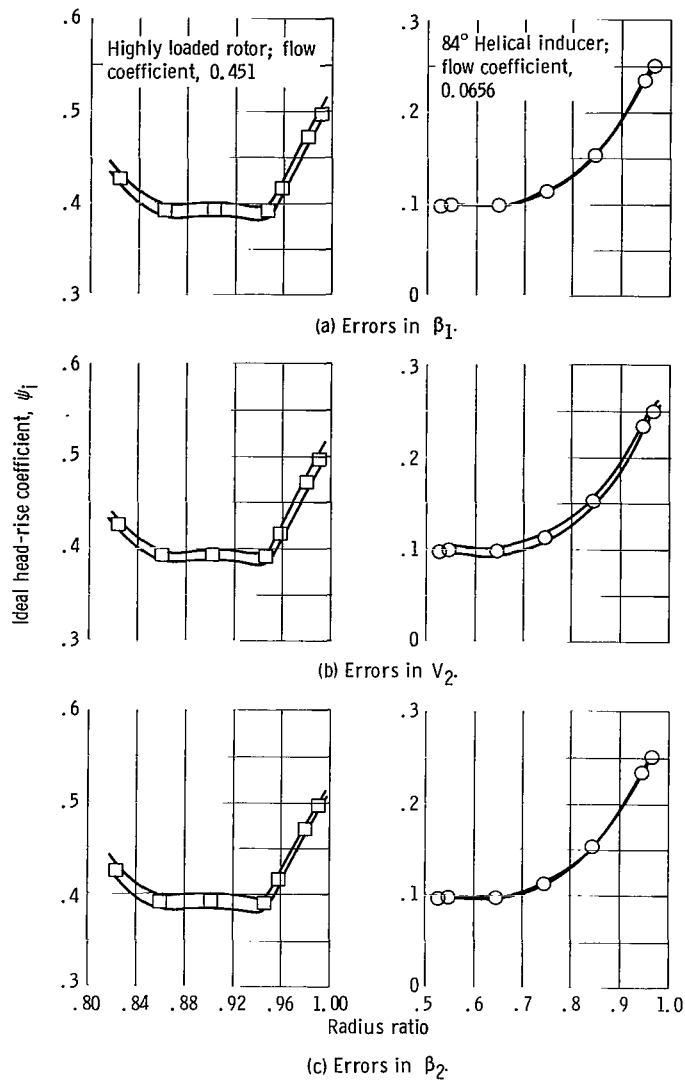


Figure 10. - Uncertainty in ideal head-rise coefficient due to measurement errors.

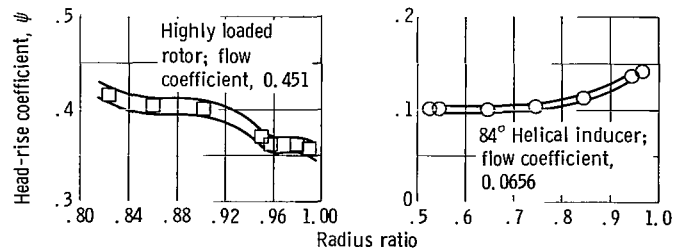


Figure 11. - Uncertainty in head-rise coefficient due to errors in head rise.

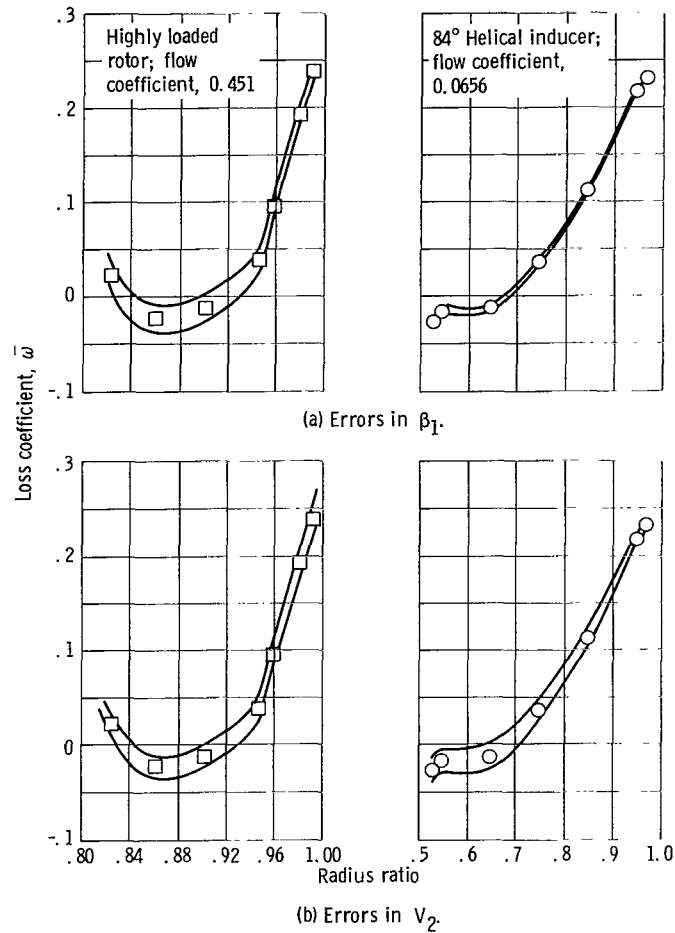
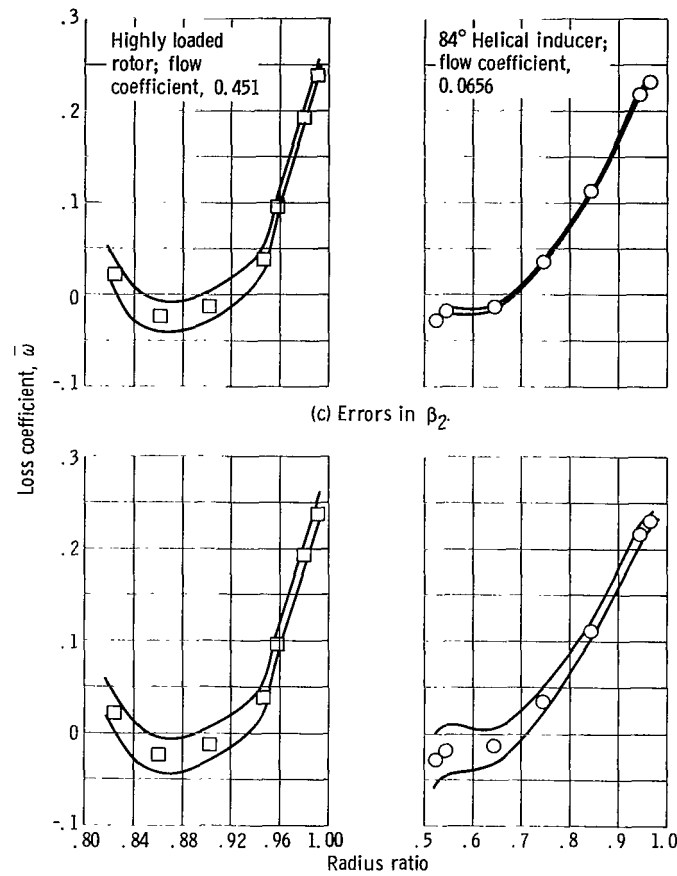


Figure 12. - Uncertainty in total pressure-loss coefficient due to measurement errors.





(c) Errors in  $\beta_2$ .

(d) Errors in  $\Delta H$ .

Figure 12. - Concluded.

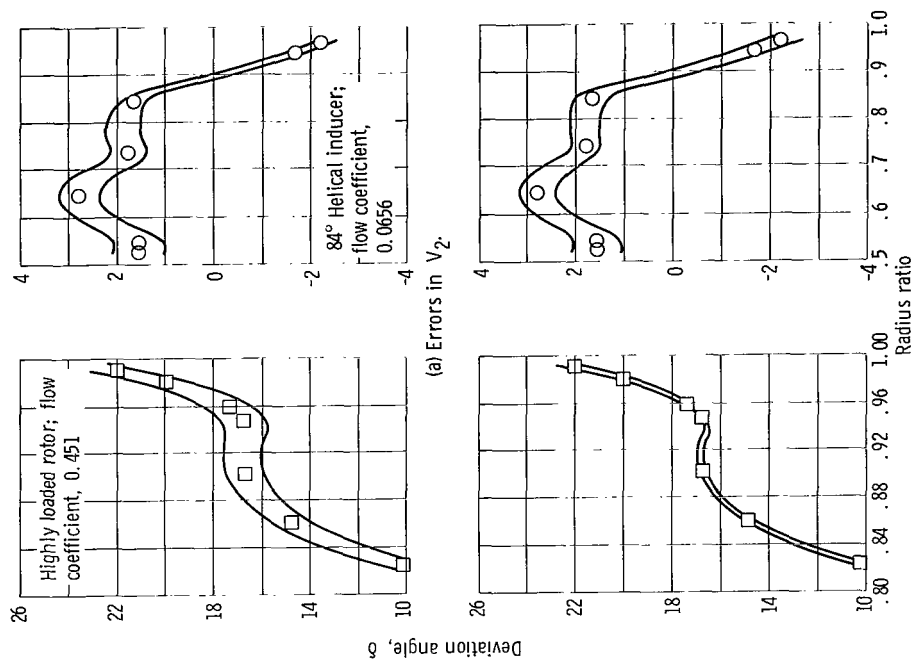


Figure 14. - Uncertainty in deviation angle due to measurement errors.

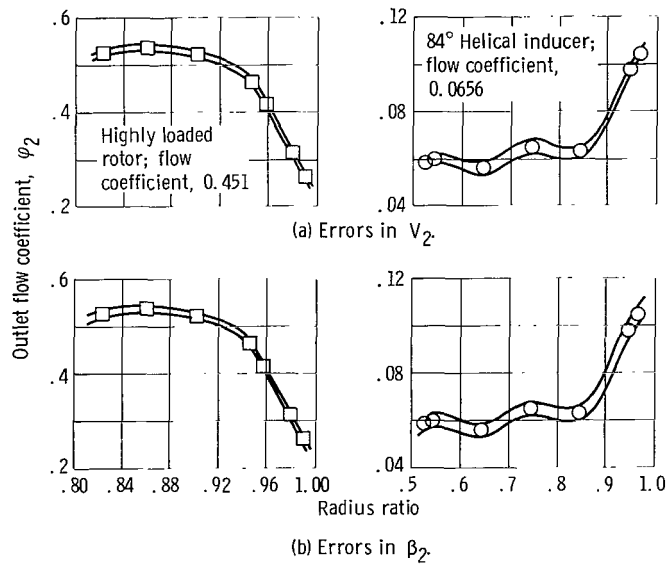


Figure 13. - Uncertainty in outlet flow coefficient due to measurement errors.

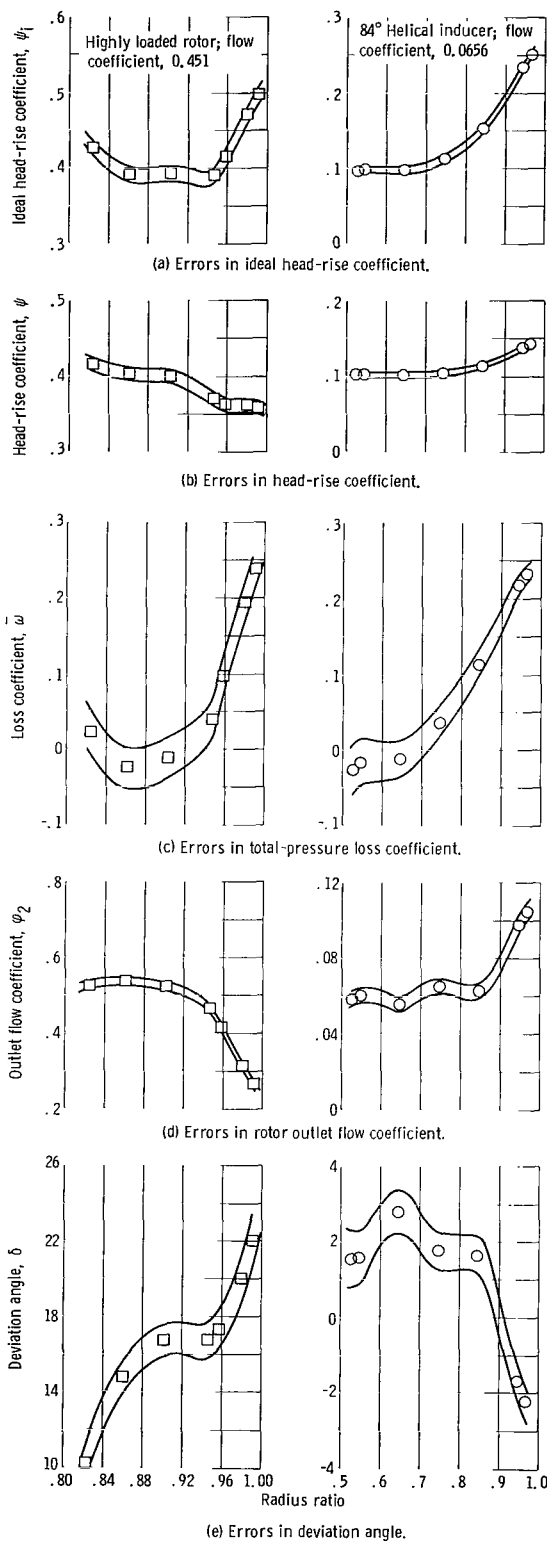


Figure 15. - Uncertainty in performance parameters due to combined effect of all measurement errors.

NATIONAL AERONAUTICS AND SPACE ADMINISTRATION  
WASHINGTON, D. C. 20546  
OFFICIAL BUSINESS

FIRST CLASS MAIL



POSTAGE AND FEES PAID  
NATIONAL AERONAUTICS AND  
SPACE ADMINISTRATION

04U 001 26 51 3DS 70195 00903  
AIR FORCE WEAPONS LABORATORY /WLOL/  
KIRTLAND AFB, NEW MEXICO 87117

ATT E. LOU BOWMAN, CHIEF, TECH. LIBRARY

POSTMASTER: If Undeliverable (Section 158  
Postal Manual) Do Not Return

*"The aeronautical and space activities of the United States shall be conducted so as to contribute . . . to the expansion of human knowledge of phenomena in the atmosphere and space. The Administration shall provide for the widest practicable and appropriate dissemination of information concerning its activities and the results thereof."*

— NATIONAL AERONAUTICS AND SPACE ACT OF 1958

## NASA SCIENTIFIC AND TECHNICAL PUBLICATIONS

**TECHNICAL REPORTS:** Scientific and technical information considered important, complete, and a lasting contribution to existing knowledge.

**TECHNICAL NOTES:** Information less broad in scope but nevertheless of importance as a contribution to existing knowledge.

**TECHNICAL MEMORANDUMS:** Information receiving limited distribution because of preliminary data, security classification, or other reasons.

**CONTRACTOR REPORTS:** Scientific and technical information generated under a NASA contract or grant and considered an important contribution to existing knowledge.

**TECHNICAL TRANSLATIONS:** Information published in a foreign language considered to merit NASA distribution in English.

**SPECIAL PUBLICATIONS:** Information derived from or of value to NASA activities. Publications include conference proceedings, monographs, data compilations, handbooks, sourcebooks, and special bibliographies.

**TECHNOLOGY UTILIZATION PUBLICATIONS:** Information on technology used by NASA that may be of particular interest in commercial and other non-aerospace applications. Publications include Tech Briefs, Technology Utilization Reports and Notes, and Technology Surveys.

*Details on the availability of these publications may be obtained from:*

SCIENTIFIC AND TECHNICAL INFORMATION DIVISION  
NATIONAL AERONAUTICS AND SPACE ADMINISTRATION  
Washington, D.C. 20546